

## Review article



# Cyclopentadienyl ring activation in organometallic chemistry and catalysis

Andrew VanderWeide & Demyan E. Prokopchuk

## Abstract

The cyclopentadienyl (Cp) ligand is a cornerstone of modern organometallic chemistry. Since the discovery of ferrocene, the Cp ligand and its various derivatives have become foundational motifs in catalysis, medicine and materials science. Although largely considered an ancillary ligand for altering the stereoelectronic properties of transition metal centres, there is mounting evidence that the core Cp ring structure also serves as a reservoir for reactive protons ( $H^+$ ), hydrides ( $H^-$ ) or radical hydrogen ( $H^\cdot$ ) atoms. This Review chronicles the field of Cp ring activation, highlighting the pivotal role that Cp ligands can have in electrocatalytic  $H_2$  production,  $N_2$  reduction, hydride transfer reactions and proton-coupled electron transfer.

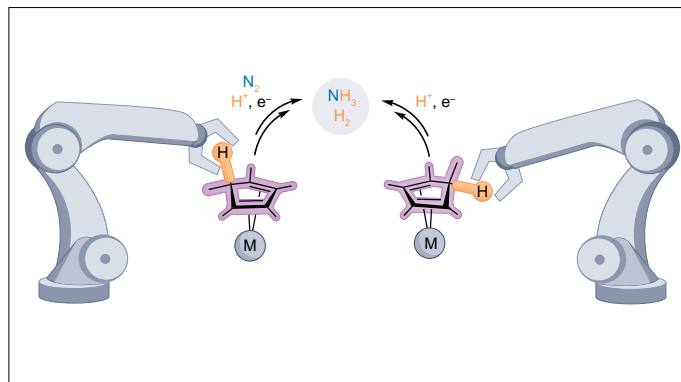
## Sections

### Introduction

### Early examples of Cp ring activation

### Implications in synthesis and catalysis

### Conclusions and future outlook



## Introduction

Ligand design has played a central role in expanding the toolbox of available transition metal complexes, with cyclopentadienyl (Cp) becoming a privileged ligand class in homogeneous catalyst development throughout the past several decades<sup>1–5</sup>. The unsubstituted Cp and its well-known electron-rich analogue pentamethylcyclopentadienyl (Cp\*) can modify the stereoelectronic properties of transition metals, usually serving as ‘innocent’ ancillary ligands that modulate reactivity at the metal centre without directly participating in bond-making and bond-breaking processes (Fig. 1). Although there are numerous literature examples showcasing the ancillary prowess of Cp and Cp\* ligands, there is an established precedent that Cp and Cp\* ligands have an active role in C–X bond activation in the presence of nucleophiles (Nu<sup>–</sup>), electrophiles (E<sup>+</sup>) or radicals (R<sup>•</sup>). In all the three cases, addition reactions to coordinatively saturated complexes containing Cp ligands disrupt the contiguous  $\eta^5$ -binding mode to generate stable and isolable  $\eta^4$ -cyclopentadiene frameworks, with *exo*-substitution being preferred in most cases.

Understanding the movement of protons and electrons by means of H<sup>+</sup>, H<sup>•</sup> and H<sup>–</sup> transfer is fundamentally important for synthetic chemistry, biology, materials science and energy-related processes. The reactivity of transition metal hydride complexes (M–H) has garnered sustained interest over the past several decades, and much has been discovered about their homolytic and heterolytic M–H bond strengths to deliver reactive H<sup>+</sup>/H<sup>•</sup>/H<sup>–</sup> moieties for applications in catalysis<sup>6–8</sup>. For example, generating reactive (weak) M–H bonds has enabled electrocatalytic H<sub>2</sub> production and oxidation<sup>9</sup>, organoradical cyclization<sup>10,11</sup>, epoxide hydrogenation<sup>12</sup> and hydrogenation of CO<sub>2</sub> to formate (HCO<sub>2</sub><sup>–</sup>)<sup>13–15</sup>. By contrast, using C–H bonds within chelating ligands such as Cp and  $\eta^4$ -cyclopentadiene (Fig. 1) to deliver reactive H<sup>+</sup>/H<sup>•</sup>/H<sup>–</sup> moieties for applications in chemical fuel synthesis and electrocatalysis remains quite rare. In this Review, we show that reactivity of the Cp manifold has long been a curiosity in organometallic chemistry by first presenting literature accounts of Cp ligand functionalization, chronologically highlighting selected examples and classifying these instances by the type of addition agent used (Nu<sup>–</sup>, E<sup>+</sup> or R<sup>•</sup>). Then, we demonstrate how since 2016 this reactivity manifold has been used for applications in chemical energy conversion such as H<sub>2</sub> production, N<sub>2</sub> reduction, proton-coupled electron transfer (PCET) and hydride transfer reactions.

## Early examples of Cp ring activation

Shortly after the discovery of ferrocene, there was a surge of interest in understanding its reactivity, preparing other metallocene derivatives and exploring the coordination chemistry of the Cp ligand in combination with other ligand types<sup>16</sup>. Although modification of the substituents surrounding the core Cp ring had become standard practice

in synthetic chemistry laboratories, it was relatively uncommon to isolate, characterize and study the reactivity of  $\eta^4$ -cyclopentadiene complexes. Herein, we focus on some early accounts of reacting Cp with nucleophiles, electrophiles and organic radicals to generate stable (and often isolable) complexes containing  $\eta^4$ -cyclopentadiene ligands coordinated to transition metals.

## Nucleophilic additions to Cp rings

Some of the earliest examples of Cp derivatization use nucleophilic reagents that attack the electrophilic Cp ring of coordinatively saturated metallocenes. The formal oxidation state of the metal decreases by 2, which is favoured by group 8 and 9 transition metals that readily undergo  $d^6 \rightarrow d^8$  electronic reconfigurations. In 1959, seminal work by Green et al.<sup>17</sup> reported the reactions of cobaltocenium or rhodocenium salts with hydride transfer agents to isolate ( $\eta^4$ -C<sub>5</sub>H<sub>6</sub>)MCp (M = Co, Rh; **1**), which were characterized by infrared (IR) and <sup>1</sup>H NMR spectroscopy (Fig. 2). In 1961, Fischer and Herberich<sup>18</sup> first reported the nucleophilic addition of phenyllithium to [Cp<sub>2</sub>Co][ClO<sub>4</sub>], generating neutral ( $\eta^4$ -C<sub>5</sub>H<sub>5</sub>Ph)CoCp (**2**). On the basis of IR spectroscopic data, this product was assigned as the *endo*- $\eta^4$ -C<sub>5</sub>H<sub>5</sub>Ph adduct; however, complex **2** was verified as the *exo* isomer by X-ray crystallography in 1964 upon combining [Cp<sub>2</sub>Co][I] with phenyllithium<sup>19</sup>. Many years later, additional spectral data for **2**, other alkyl derivatives, alkoxides, amides and phosphides indicated that *exo*-substitution occurred in practically all cases<sup>20</sup>. In 1961, Wilkinson and co-workers<sup>21</sup> extended their work to piano-stool (that is, half-sandwich) iron complexes, in which [CpFe(CO)<sub>2</sub>PPPh<sub>3</sub>]<sup>+</sup> was treated with sodium borohydride to generate ( $\eta^4$ -C<sub>5</sub>H<sub>6</sub>)Fe(CO)<sub>2</sub>PPPh<sub>3</sub> (**3**) and characterized by IR and <sup>1</sup>H NMR spectroscopy. The rhodium variant, (*exo*- $\eta^4$ -C<sub>5</sub>H<sub>5</sub>Ph)RhCp, was reported 2 years later<sup>22</sup>. In 1978, these nucleophilic addition patterns were framed in a broader context as part of the Davies–Green–Mingos rules for nucleophilic addition to unsaturated hydrocarbon ligands<sup>23</sup>. Decades later, the electrophilic character of the cobaltocenium cation was ‘rediscovered’ to generate other *exo*-substituted  $\eta^4$ -C<sub>5</sub>H<sub>4</sub>R derivatives<sup>24–26</sup>. For example, the complex (*exo*- $\eta^4$ -C<sub>5</sub>H<sub>5</sub>C≡C(SiMe<sub>3</sub>))CoCp (**4**) was prepared by Tang and co-workers by reacting [Cp<sub>2</sub>Co][PF<sub>6</sub>]<sup>–</sup> with lithium trimethylsilyl acetylide. Complex **4** was then used as a building block to prepare monomers via azide–alkyne ‘click’ chemistry to make metallocopolymers (**5**), which was later extended to rhodocenes<sup>27</sup>. Shortly afterwards, Bildstein and co-workers independently published a very similar pathway to prepare complex **4** as a synthon for the preparation of cobaltocenium carboxylic acid<sup>28</sup>. Very recently, Cp\* ring activation with an Ir<sup>III</sup> cation was found to be strongly dependent on the identity of the carbon-based nucleophile<sup>29</sup>. In summary, the *exo*-addition of nucleophiles to Cp and Cp\* has been firmly established; however, the release of H<sup>–</sup> (that is, the reverse reaction) has only been applied in recent years for the reduction of small molecules such as NAD<sup>+</sup> and CO<sub>2</sub>.

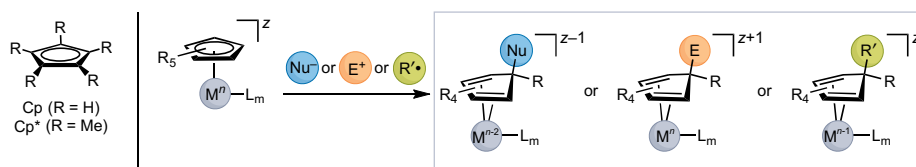


**Fig. 1 | The active role of Cp ligands in transition metal complexes.** Possible reaction outcomes via activation of cyclopentadiene ligands using nucleophiles (Nu<sup>–</sup>), electrophiles (E<sup>+</sup>) or radicals (R<sup>•</sup>), which are the focus of this Review. R<sub>5</sub>

represents cyclopentadienyl (Cp), Cp\* and other substituted Cp analogues. L<sub>m</sub>, coordinating ligand (ligands); M, transition metal; n, oxidation state; Z, overall charge.

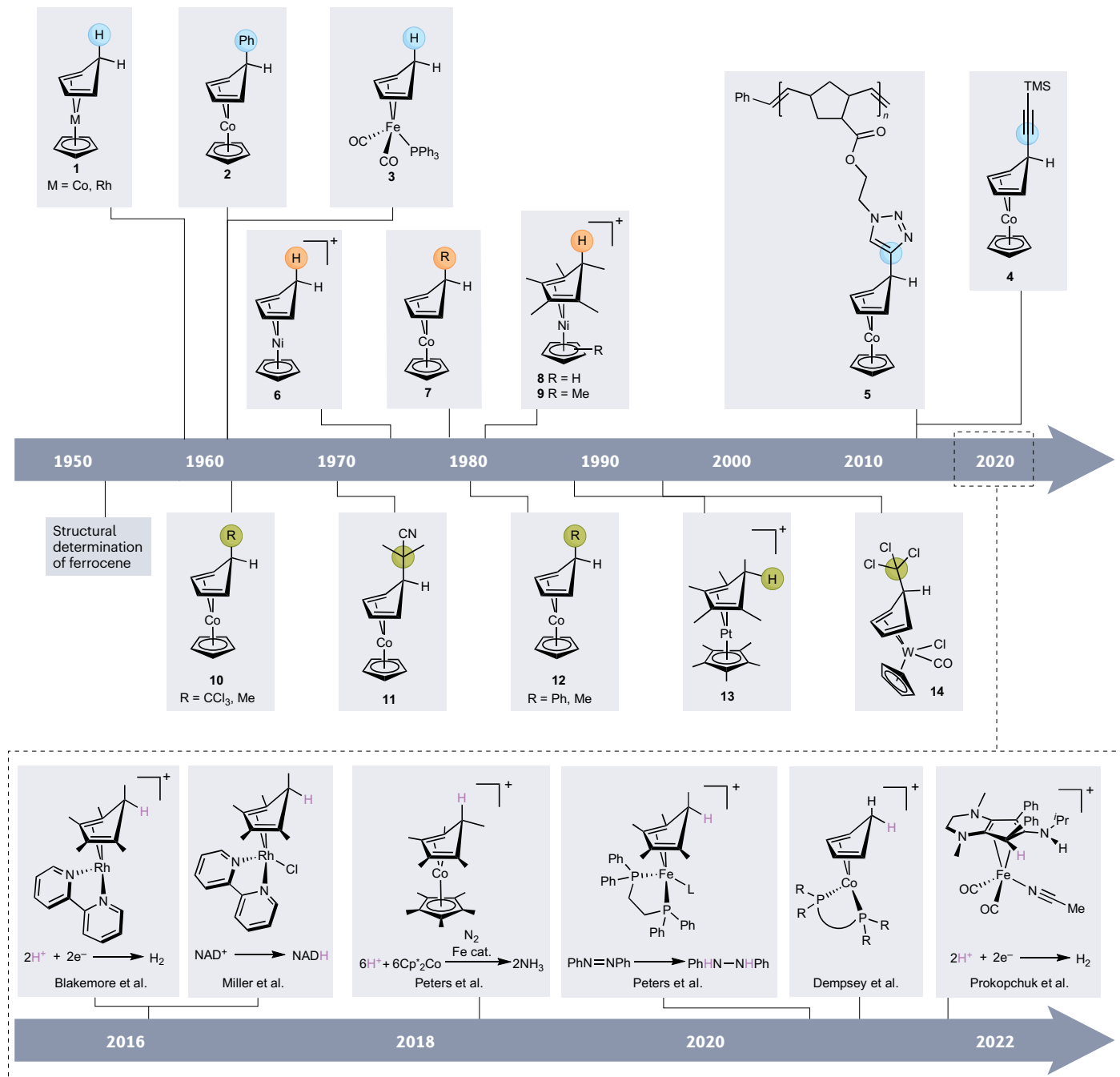


**Fig. 2 | Discovery timeline of selected ring-activated cyclopentadiene complexes.** The top section shows selected ring activation examples before 2016, in which the  $\eta^5$ -cyclopentadienyl ring is attacked by nucleophiles, electrophiles or radicals. Complexes 1–5 were synthesized via nucleophilic addition (blue)<sup>17–28</sup>, complexes 6–9 were synthesized via electrophilic addition (orange)<sup>34–38,89</sup>,

and complexes 10–14 were synthesized via radical addition (yellow)<sup>17,37,39–47</sup>. The lower box shows the resurgence of interest in cyclopentadienyl ring activation from 2016 onwards, which involves the net transfer of  $\text{H}^+$ ,  $\text{H}^-$  or  $\text{H}^\pm$  to/from small molecules<sup>91,95–97,107,122–124,129,132,134</sup>. TMS, trimethylsilyl.

## Electrophilic additions to Cp rings

The discovery of electrophilic substitution reactions with ferrocene opened new vistas of organometallic chemistry in the twentieth century<sup>30–32</sup>. It is widely accepted that Cp ring activation by the

incoming electrophile ( $\text{E}^+$ ) occurs before loss of  $\text{H}^+$ , generating a transient  $[(\eta^4\text{-C}_5\text{H}_4\text{E})\text{FeCp}]^+$  intermediate<sup>31,33</sup>. In later years, electrophilic addition products were reported with electron-rich metallocenes that formally have 20 valence electrons, which make the Cp ligands more susceptible

to electrophilic attack. In 1974, the protonation of nickelocene was achieved by treating it with anhydrous HF, which allowed for the spectroscopic detection of  $[(\eta^4\text{-C}_5\text{H}_6)\text{NiCp}]^+$  (**6**) by  $^1\text{H}$  NMR spectroscopy with a proposed  $\text{F}^-$  or  $[\text{HF}]^-$  counterion<sup>34</sup> (Fig. 2). However, attempts to isolate this complex with a  $[\text{BF}_4]^-$  counterion led to diene loss and the formation of  $[\text{CpNi}][\text{BF}_4]$ . In 1975 and 1976, reports of the electro-generated anion  $[\text{Cp}_2\text{Co}]^-$  reacting with carbon-based electrophiles  $\text{RX}$  ( $\text{R} = \text{CH}_2\text{Ph}, \text{CHClPh}, \text{CCl}_3, \text{CH}_2\text{Br}$ ) to furnish the neutral (*exo*- $\eta^4\text{-C}_5\text{H}_5\text{R}$ )  $\text{CoCp}$  (**7**) in high yield were published<sup>35,36</sup>. Interestingly,  $\text{CO}_2$  also reacts with  $[\text{Cp}_2\text{Co}]^-$  to generate a proposed (unstable) ring-activated carboxylate anion  $[(\text{exo-}\eta^4\text{-C}_5\text{H}_5\text{CO}_2)\text{CoCp}]^-$  that is converted to the isolable ester (*exo*- $\eta^4\text{-C}_5\text{H}_5\text{CO}_2\text{Me}$ )  $\text{CoCp}$  by reaction with methyl iodide. In 1980, the synthesis of  $[(\text{exo-}\eta^4\text{-C}_5\text{Me}_5\text{R})\text{NiCp}]^*[\text{BF}_4]$  (**9**) from nickelocene was reported using several different alkyl and aryl electrophiles, which were suggested to be *exo*-products owing to the similar chemical shifts for all the *endo*-methyl resonances via  $^1\text{H}$  NMR spectroscopy<sup>37</sup>. In the same year, it was shown that  $\text{HBF}_4$  selectively protonates the electron-rich  $\text{Cp}^*$  ligand of  $\text{Cp}^*_2\text{Ni}$  and  $\text{Cp}^*\text{NiCp}$  to yield the stable  $[(\eta^4\text{-C}_5\text{Me}_5\text{H})\text{NiCp}]^*[\text{BF}_4]$  and  $[(\eta^4\text{-C}_5\text{Me}_5\text{H})\text{NiCp}]^*[\text{BF}_4]$  (**8**); however, *exo*-protonation versus *endo*-protonation was structurally ambiguous<sup>38</sup>. As described in the sections covering  $\text{N}_2$  reduction and stoichiometric PCET, protonation of a paramagnetic metallocene yields an isolable ring-activated product that releases  $\text{H}^+$ , whereas  $\text{Cp}$  protonation of diamagnetic piano-stool complexes precedes ligand-to-metal proton migration reactions. These types of electrophilic addition reactions are relevant to (electro)catalytic  $\text{NH}_3$  formation and  $\text{H}_2$  production, respectively, under reducing conditions.

## Radical additions to $\text{Cp}$ rings

Radical-based addition reactions of haloalkanes to  $\text{Cp}$ -containing complexes have been primarily investigated with cobaltocene ( $\text{Cp}_2\text{Co}$ ), a paramagnetic metallocene that formally possesses 19 valence electrons. In 1956, Wilkinson et al.<sup>39</sup> observed that  $\text{Cp}_2\text{Co}$  reacts with bromoethane to generate the diamagnetic cobaltocenium bromide, however the fate of the alkyl moiety was unclear. Subsequently, reactions with other haloalkanes were reported (MeI,  $\text{CCl}_4$ ), and  $\text{Cp}_2\text{Co}$  disproportionates to afford (*exo*- $\eta^4\text{-C}_5\text{H}_5\text{R}$ )  $\text{Co}^*\text{Cp}$  (**10**) (Fig. 2) and an equivalent of  $[\text{Cp}_2\text{Co}^{\text{III}}][\text{X}]$  ( $\text{X} = \text{I}, \text{Cl}$ ), as evidenced by IR and  $^1\text{H}$  NMR spectroscopy<sup>17,40</sup>. Starting in 1969, a series of papers were published that discovered a radical addition mechanism to form such *exo*-alkylation products. Kinetic studies showed that the rate of  $\text{Cp}_2\text{Co}$  alkylation expectedly increases with better leaving group halogen ( $\text{Cl} > \text{Br} > \text{I}$ ) and rates increase when the halomethyl group has one, two or three halogen atoms, respectively<sup>41</sup>. In 1970, the reaction of  $\text{Cp}_2\text{Co}$  with the radical initiator azoisobutyronitrile afforded nearly quantitative amounts of (*exo*- $\eta^4\text{-C}_5\text{H}_5(\text{C}(\text{CH}_3)_2\text{CN})$ )  $\text{CoCp}$  (**11**), demonstrating that  $\text{Cp}_2\text{Co}$  is an effective radical trap<sup>42</sup>. Follow-up kinetic studies further supported these claims, showing that an initial electron transfer step to generate  $[\text{Cp}_2\text{Co}^{\text{III}}]^+$  and  $\text{R}^\cdot$  is rate-limiting<sup>43,44</sup>. The electron-rich  $\text{Cp}^*_2\text{Co}$  reacts similarly with  $\text{CH}_3\text{I}$  and  $\text{C}_6\text{H}_5\text{I}$  to generate diamagnetic (*exo*- $\eta^4\text{-C}_5\text{Me}_5\text{R}$ )  $\text{CoCp}^*$  (**15**) and  $[\text{Cp}^*_2\text{Co}][\text{I}]$ <sup>37</sup>. In 1994, the platinum adduct  $[(\text{endo-}\eta^4\text{-C}_5\text{Me}_5\text{H})\text{PtCp}^*][\text{BF}_4]$  (**13**) was reported to undergo oxidation via controlled potential electrolysis to produce the  $\text{Pt}^{\text{IV}}$  metallocene dication  $[\text{Cp}^*_2\text{Pt}]^{2+}$ ; however, the fate of released  $\text{H}^+$  remained unclear<sup>45</sup>. Controlled potential electrolysis of the resultant  $[\text{Cp}^*_2\text{Pt}]^{2+}$  under reducing conditions regenerates  $[(\eta^4\text{-C}_5\text{Me}_5\text{H})\text{PtCp}^*]^+$ , with solvent or decomposition product (products) possibly acting as  $\text{H}^+$  sources<sup>46</sup>. In 1996, the isolation and structural characterization of (*exo*- $\eta^4\text{-C}_5\text{H}_4\text{CCl}_3$ )  $\text{WCp}(\text{Cl})(\text{CO})$  (**14**) was achieved by reaction of

$\text{Cp}_2\text{W}(\text{CO})$  with a large excess of  $\text{CCl}_4$ , and it was proposed that initial *exo*-attack of a trichloromethyl radical on the  $\text{Cp}$  ring was followed by chloride addition to the metal centre<sup>47</sup>. In recent years, addition reactions using organoradicals have garnered much less attention, but the release of  $\text{H}^+$  from  $\eta^4\text{-CpH}$  ligands has become important, as described in the sections below on  $\text{N}_2$  reduction and stoichiometric PCET.

## Other instances of $\text{Cp}$ ring activation

Other reports of  $\text{Cp}$  ring activation do not cleanly fit into one of the aforementioned reactivity classes. For instance, other hapticity changes (that is, ring slippage to  $\eta^3\text{-Cp}$  or  $\eta^1\text{-Cp}$ ) can accompany ring activation; this subject has been reviewed elsewhere<sup>48</sup>. In some cases, ring-activated molecules are isolated as unexpected by-products and/or characterized to varying degrees<sup>49–53</sup>, whereas in other cases, the exact reaction conditions that lead to ring activation are unclear<sup>54–57</sup>. Ring-activated complexes can also be isolated as products of intramolecular insertion reactions, in which a coordinatively saturated metal complex bears a ligand capable of inserting into the  $\text{Cp}-\text{M}$  bond, driven to form an  $\eta^4\text{-C}_5\text{H}_4\text{R}$  moiety in the presence of excess ligand and UV<sup>58</sup> or visible<sup>59</sup> light. Electronic effects at the metal centre<sup>60–62</sup> or the influence of cluster ligands<sup>63–67</sup> can also lead to cases in which  $\eta^4$ -coordination is preferred over  $\eta^5$ -coordination. Ring-activated complexes have also been proposed as transient reaction intermediates involving *f*-block metallocenes<sup>68</sup> and to explain deuterium incorporation into the  $\text{Cp}$  ligand<sup>69–71</sup>. Notably, the reactivity of alkyl substituents on  $\text{Cp}$  ligands to generate fulvenes<sup>72–74</sup> and of  $\eta^6\text{-C}_6\text{Me}_6$  ligands on  $\text{CpFe}$  sandwich complexes<sup>75</sup> are beyond the scope of this Review.

## Implications in synthesis and catalysis

The remainder of this Review focuses on the resurgence of  $\text{Cp}$  ring activation chemistry from 2016 onwards, where perturbation of the aromatic ring structure to form  $\eta^4\text{-CpH}$  moieties becomes essential to mediate the delivery of  $\text{H}^+$ ,  $\text{H}^-$  or  $\text{H}^\cdot$  to produce  $\text{H}_2$ ,  $\text{NH}_3$  and reduced organic molecules (Fig. 2, bottom). In particular,  $\text{H}_2$  and  $\text{NH}_3$  are essential commodity chemicals for the agriculture enterprise to support our current global population, and their sustainable production will have a central role in minimizing global  $\text{CO}_2$  emissions<sup>76</sup>. Furthermore, understanding the kinetic and thermochemical requirements for rapidly and efficiently moving hydrogen using the  $\eta^4\text{-Cp}$  ring system has broad implications in developing new catalysts that mediate PCET reactions<sup>77</sup>.

## $\text{H}_2$ production

The sustainable and economical production of  $\text{H}_2$  is an essential component of converting solar energy into chemical fuels<sup>78</sup>. Many groups have taken inspiration from hydrogenases<sup>79,80</sup>, placing amine bases capable of shuttling protons to the metal in the secondary coordination sphere to increase the efficacy of hydrogen production catalysis<sup>9,81</sup>. Complexes with the general formula  $[\text{Cp}^*\text{Rh}^{\text{III}}\text{L}(\text{bpy})]^{2+}$  ( $\text{bpy} = 2,2'\text{-bipyridine}$ ,  $\text{L} = \text{H}_2\text{O}$  or  $\text{MeCN}$ ) are well-known precatalysts for various reactions such as reduction of  $\text{NAD}^+$  (refs. 82–84), oxidation of formate<sup>85,86</sup> and the reduction of  $2\text{H}^+$  to  $\text{H}_2$  (refs. 87,88). The hydrogen production reactions were believed to proceed through a well-accepted mechanism that first involves  $2\text{e}^-$  reduction of  $[\text{Cp}^*\text{Rh}^{\text{III}}(\text{NCMe})(\text{bpy})]^{2+}$  (**20**) to furnish the electron-rich  $\text{Cp}^*\text{Rh}^{\text{I}}(\text{bpy})$  (**15**), followed by protonation to give hydride complex  $\text{Cp}^*\text{Rh}^{\text{II}}\text{H}(\text{bpy})$  (**18**), followed by electrophilic attack of  $\text{Rh-H}$  moiety with a second proton to generate  $\text{H}_2$  (ref. 87) (Fig. 3). Evidence in support of this mechanism first included  $^1\text{H}$  NMR spectroscopic observation of complex **15** (ref. 89), followed by the synthesis and crystallographic characterization of complex **15** in high yield<sup>90</sup>.

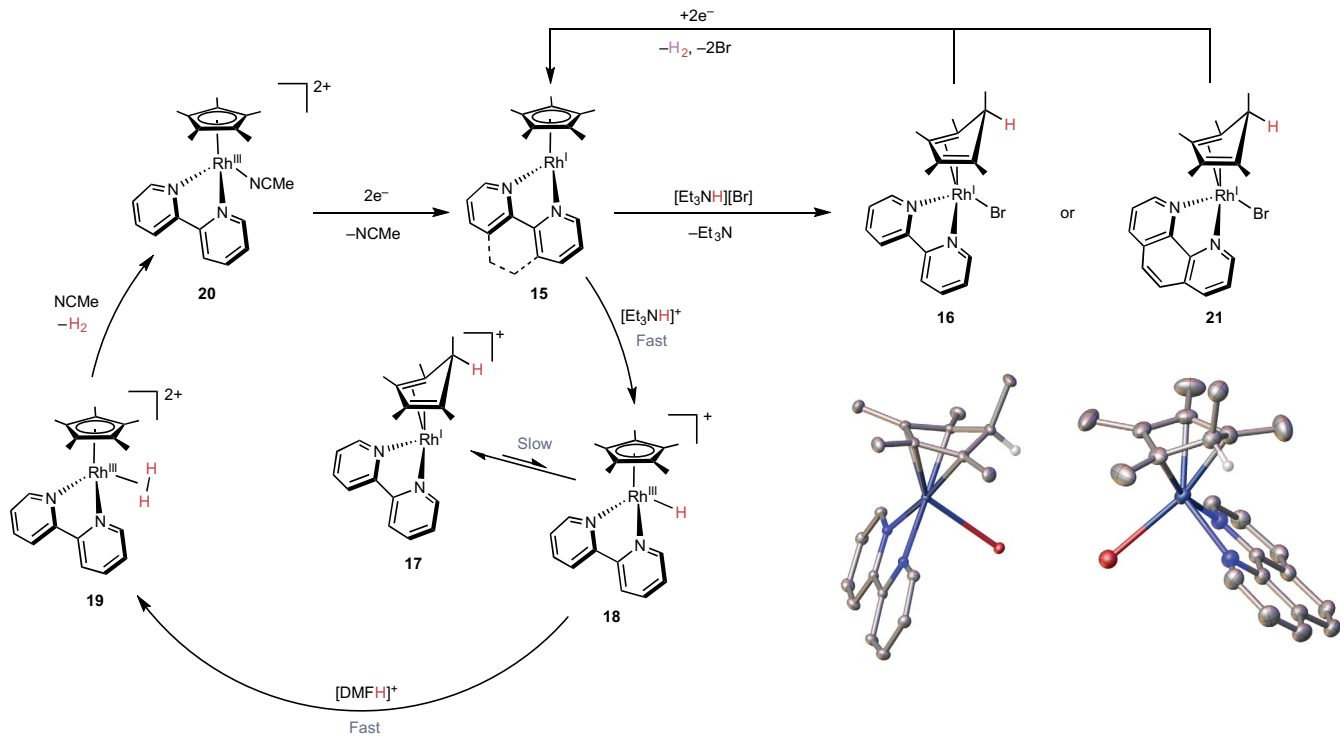


**Fig. 3 | Cyclopentadiene ring activation in H<sub>2</sub> production using [Cp\*Rh<sup>III</sup>(NCMe)(bpy)]<sup>+</sup> catalysts.** The 2e<sup>-</sup> reduction of complex **20** enables ligand protonation by  $[\text{Et}_3\text{NH}]^+[\text{Br}]$ , generating ring-activated complexes **16** or **21** (phenanthroline derivative), which have been characterized by single-crystal X-ray diffraction (CCDC 1424707 (**16**) and 1546016 (**21**))<sup>91,96</sup>. Using  $[\text{Et}_3\text{NH}]^+$  with

a weakly coordinating anion generates off-cycle complex **17** via transient metal hydride intermediate **18** (refs. 91,95). Reacting **17/18** with strong acids such as  $[\text{DMFH}]^+$  results in H<sub>2</sub> evolution and regeneration of **20**. **bpy**, 2,2'-bipyridine; **Cp<sup>\*</sup>**, pentamethylcyclopentadienyl;  $[\text{DMFH}]^+$ , *N,N'*-dimethylformamidinium.

In 2016, Blakemore et al. reported that Cp<sup>\*</sup>Rh<sup>I</sup>(bpy) (**15**) behaves as a chemically non-innocent Cp<sup>\*</sup> ligand coordinated to Rh, forming an  $\eta^4$ -Cp<sup>\*</sup>H intermediate that might have a role in catalytic H<sub>2</sub> evolution<sup>91</sup> (Fig. 3). Established conditions for catalytic H<sub>2</sub> production using complex **15** require strongly acidic conditions<sup>87,88</sup>, and exposure of complex **15** to excess *N,N*-dimethylformamidinium trifluoromethanesulfonate ( $[\text{DMFH}]^+[\text{OTf}]$ ;  $\text{pK}_a^{\text{MeCN}} = 6.1$ )<sup>92</sup> releases a stoichiometric amount of H<sub>2</sub>, as measured by gas chromatography. Switching to weaker acids not only lowered the driving force for H<sub>2</sub> evolution<sup>93</sup> but also offered the possibility of isolating catalytically relevant intermediates if the acid is strong enough to react with the electron-rich catalyst but too weak to generate H<sub>2</sub>. When Cp<sup>\*</sup>Rh<sup>I</sup>(bpy) is exposed to  $[\text{Et}_3\text{NH}]^+[\text{Br}]$  ( $\text{pK}_a^{\text{MeCN}} = 18.8$ )<sup>94</sup>, a colour change is observed but no H<sub>2</sub> is released. This crucial reaction enabled the isolation and X-ray crystallographic characterization of (*endo*- $\eta^4$ -C<sub>5</sub>Me<sub>5</sub>H)Rh<sup>I</sup>Br(bpy) (**16**), in which the proton is located *endo*-orientation relative to the metal centre (Fig. 3, right). The bromide-free salt (*endo*- $\eta^4$ -C<sub>5</sub>Me<sub>5</sub>H)Rh<sup>I</sup>(bpy) (**17**) was characterized via NMR spectroscopy by instead using  $[\text{Et}_3\text{NH}]^+[\text{OTf}]$  as the acid source. Importantly, exposure of these *endo*- $\eta^4$ -C<sub>5</sub>Me<sub>5</sub>H complexes to excess  $[\text{DMFH}]^+[\text{OTf}]$  cleanly releases H<sub>2</sub> and produces [Cp<sup>\*</sup>Rh<sup>III</sup>(L)(bpy)]<sup>+</sup> (**20**), in which L is the coordinated solvent (MeCN) or conjugate base (DMF).

The protonation behaviour of Cp<sup>\*</sup>Rh<sup>I</sup>(bpy) was probed by ground-state density functional theory (DFT) studies<sup>91,95</sup>. When complex **15** reacts with a weaker acid,  $[\text{Et}_3\text{NH}]^+$ , the metal is first protonated to give complex **18**, which then isomerizes to the more stable complex **17**.

These results are all consistent with the observation of exclusive *endo*-selectivity in the presence of  $[\text{Et}_3\text{NH}]^+$ . The lowest computed energy pathway requires tautomerization from the ligand to the metal before protonation of complex **18** to generate transient dihydrogen-bound complex **19**. In summary, these computational findings showed that [*(endo*- $\eta^4$ -C<sub>5</sub>Me<sub>5</sub>H)Rh<sup>I</sup>(bpy)]<sup>+</sup> (**17**) is an off-cycle thermodynamic sink during H<sub>2</sub> production, which can be avoided in the presence of strong acids owing to the kinetically favourable sequential protonation of the Rh<sup>I</sup> metal centre and Rh<sup>III</sup>-H intermediate<sup>95</sup>.

Conjugated N-donor ligands beyond 2,2'-bipyridine can also be used for stoichiometric and electrocatalytic H<sub>2</sub> production<sup>96,97</sup>. The structurally authenticated complex (*endo*- $\eta^4$ -C<sub>5</sub>Me<sub>5</sub>H)Rh<sup>I</sup>Br(phen) (phen = phenanthroline; **21**) was synthesized, and its electrochemical behaviour was interrogated<sup>96</sup> (Fig. 3, right). Controlled potential electrolysis experiments with complex **21** (or isostructural complex **16**) produced 1 equiv. H<sub>2</sub>, underscoring that H<sub>2</sub> evolution is feasible in the absence of exogenous acid. Electronic modifications at the 4,4' positions of the bipyridine ligand (bpy<sup>R</sup> where R = <sup>3</sup>Bu, H or CF<sub>3</sub>) were conducted and compared with the reactivity of **15** (ref. 97). Controlled potential electrolysis verified that H<sub>2</sub> is produced in catalytic amounts, with a maximum turnover number of 4.4. Post-electrolysis solutions using [Cp<sup>\*</sup>Rh<sup>III</sup>Br(bpy<sup>CF<sub>3</sub></sup>)]<sup>+</sup> reveal a large build-up of the protonated solvent adduct (*(endo*- $\eta^4$ -C<sub>5</sub>Me<sub>5</sub>H)Rh<sup>I</sup>(NCMe)(bpy<sup>CF<sub>3</sub></sup>)]<sup>+</sup>, implying that it is a plausible (off-cycle) resting state during electrocatalysis. Collectively, these observations suggest that electronic modifications to the ancillary ligand environment do not enhance catalytic

performance and cast further doubt on the relevance of  $\text{Cp}^*$  ring activation with these Rh-based systems.

The sluggish catalytic activity reactivity of the precious metal complexes described above indicates that they are economically and environmentally impractical to meet demands for sustainable  $\text{H}_2$  on a scale suitable for chemical energy production<sup>98</sup>. Iron is the most abundant transition metal in the upper crust of the Earth and represents an ideal alternative; however, the library of synthetically tractable  $\text{CpFe}$ -based  $\text{H}_2$  production or  $\text{H}_2$  oxidation electrocatalysts remains limited<sup>99–104</sup> and none rival the efficiency and speed of  $[\text{FeFe}]$ -hydrogenase (less than 0.1 V overpotential and turnover frequency of 6,000–9,000 s<sup>-1</sup> for  $\text{H}_2$  production)<sup>80,105,106</sup>. Thus, there is still great interest in designing Earth-abundant  $\text{H}_2$  production catalysts, particularly with systems that incorporate biomimetic primary or secondary coordination sphere modifications to facilitate proton shuttling to/from the metal centre<sup>9,79,105</sup>. In 2021, Prokopchuk and co-workers reported tri-amine-functionalized piano-stool Fe complexes [<sup>en</sup> $\text{Cp}^R\text{Fe}(\text{NCMe})(\text{CO})_2$ ]<sup>+</sup> ( $\text{en} = \text{N,N}'\text{-dimethylethylenediamine}$ ,  $R = \text{NH}^+\text{Pr}$ , Pyrr, NBn) as proton reduction electrocatalysts to form  $\text{H}_2$ , with the  $^i\text{Pr}$  variant [<sup>en</sup> $\text{Cp}^{\text{NH}^i\text{Pr}}\text{Fe}(\text{NCMe})(\text{CO})_2$ ]<sup>+</sup> (**22**)<sup>107</sup> shown in Fig. 4. All three solvent adducts catalyse the production of  $\text{H}_2$  in acetonitrile using  $\text{Tos}_2\text{NH}$  as the proton source with maximum  $\text{H}_2$  production catalytic rates of 29–45 s<sup>-1</sup>.

The reaction mechanism was rationalized via state-of-the-art DFT approaches<sup>108</sup> using [<sup>en</sup> $\text{Cp}^{\text{NH}^i\text{Pr}}\text{Fe}(\text{NCMe})(\text{CO})_2$ ]<sup>+</sup> (**22**)<sup>107</sup> (Fig. 4). The delivery of  $2\text{H}^+$  and  $2\text{e}^-$  to complex **22** can occur in several different permutations before  $\text{H}_2$  evolution, which include protonation at many possible sites as highlighted in blue for the structure of complex **22**. The most thermochemically reasonable pathway after  $1\text{e}^-$  reduction was found to be *endo*-selective protonation at the  $\text{Cp}$  ring (**23**) based on its computed acidity ( $\text{pK}_a^{\text{MeCN}} = 15.7$ ) relative to exogenous acid  $\text{Tos}_2\text{NH}$  ( $\text{pK}_a^{\text{MeCN}} = 11.97$ )<sup>109</sup>, whereas protonation at the  $\text{NH}^i\text{Pr}$  moiety (**25**) was deemed unlikely on thermochemical grounds ( $\text{pK}_a^{\text{MeCN}} = 8.9$ ). Steric arguments presumably make *exo*-protonation at the <sup>en</sup> $\text{Cp}^{\text{NH}^i\text{Pr}}$  ring significantly less favourable ( $\text{pK}_a^{\text{MeCN}} = 5.4$ ), and direct protonation of the

metal centre (**24**) is also implausible owing to the higher computed acidity of the resultant  $\text{Fe}^{\text{III}}\text{-H}$  intermediate ( $\text{pK}_a^{\text{MeCN}} = 9.6$ ). Reduction of the solvent-coordinated intermediate  $[(\text{endo-}\eta^4\text{-en}\text{CpH})\text{Fe}(\text{NCMe})(\text{CO})_2]^+$  ( $E^\circ = -1.01$  V) followed by solvent dissociation and ligand-to-metal proton migration was proposed to yield a stable  $\text{Fe}^{\text{II}}\text{H}$  complex (**26**). Finally, complex **26** was proposed to undergo direct protonation by exogenous acid to yield complex **27**, followed by  $\text{H}_2$  release. Overall, these data indicated that the amines were chemically innocent during electrocatalysis, and ligand-to-metal proton migration was essential for electrocatalytic  $\text{H}_2$  evolution, contrasting with the inhibitory tautomerization behaviour of the  $\text{Cp}^*\text{Rh}^i(\text{bpy})$  complexes described earlier. Therefore, amine-functionalized  $\text{Cp}$  ligands coordinated to Earth-abundant metals exhibit unique chemically non-innocent reactivity patterns under electrochemical bias, and the kinetic details for these elementary reaction steps warrant deeper investigation.

## $\text{N}_2$ reduction

There have been widespread efforts to develop homogeneous and heterogeneous catalysts for the efficient conversion of  $\text{N}_2$  to  $\text{NH}_3$  (ref. 110), particularly in processes that minimize the use of fossil fuel feedstocks to circumvent the need for centralized Haber–Bosch production facilities<sup>76</sup>. To date, no molecular catalysts have been reported that directly convert gaseous  $\text{H}_2$  and  $\text{N}_2$  into  $\text{NH}_3$ ; therefore, powerful reductants ( $E^\circ \leq -1.3$  V versus  $\text{Fc}^{+/0}$ ) and strong acids ( $\text{pK}_a^{\text{THF}} \leq 8$ ) dissolved in organic solvent are commonly used in molecular catalysis to achieve catalytic turnovers in the  $\text{N}_2$  reduction reaction ( $\text{N}_2\text{RR}$ ), with particular attention focused on minimizing  $\text{H}_2$  evolution by metering the amount of available  $\text{H}^+/\text{e}^-$  in solution<sup>111–115</sup>. In recent years, researchers have made progress towards increasing molecular  $\text{N}_2\text{RR}$  efficiency by surveying PCET reagents that minimize the thermochemical driving force for this  $6\text{H}^+/\text{e}^-$  reaction<sup>77,116–118</sup>. In 2017, Peters and co-workers recognized that some of the most active molecular  $\text{N}_2\text{RR}$  catalysts use  $\text{Cp}_2\text{Co}$  or  $\text{Cp}^*\text{Co}$  as  $1\text{e}^-$  reductants in the presence of strong acid to generate  $\text{NH}_3$  and/or  $\text{N}_2\text{H}_4$  (refs. 111,112,119–121) and postulated that metallocenes might play a chemically non-innocent role<sup>122</sup>. Compelling DFT calculations

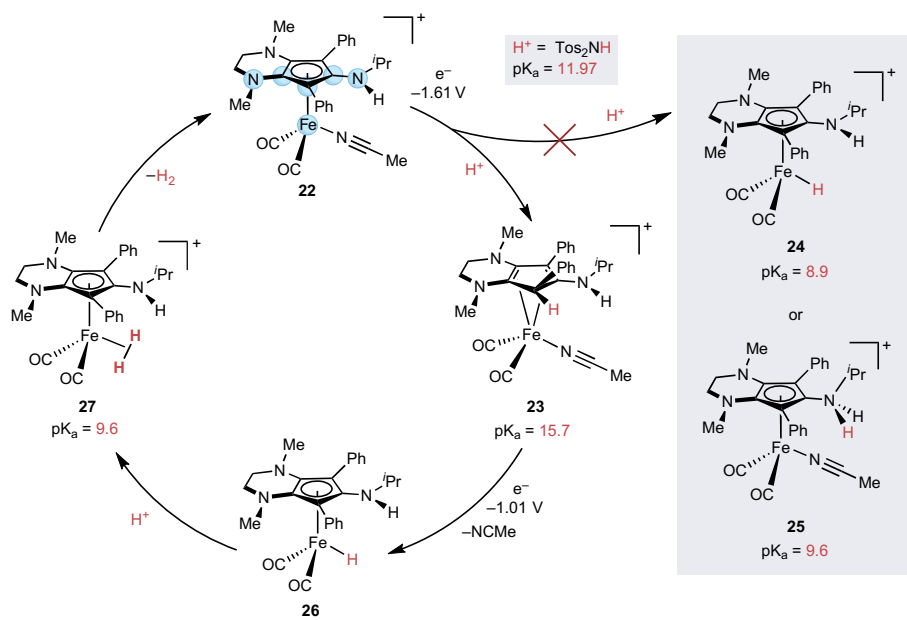
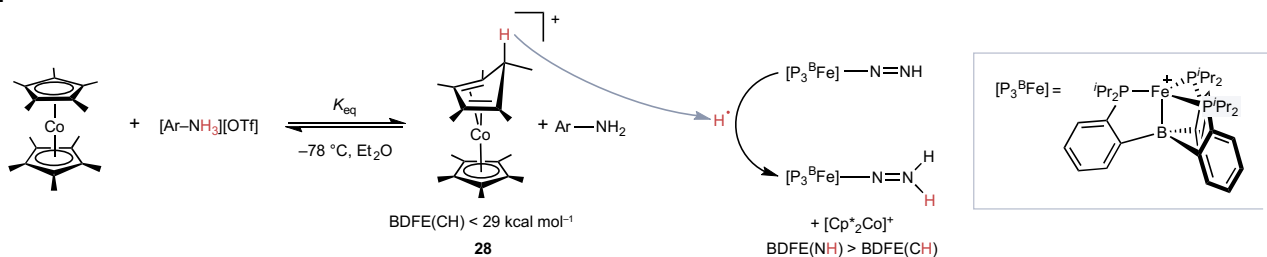


**Fig. 4 | Proposed *endo*-selective protonation and ligand-to-metal proton migration during  $\text{H}_2$  production using [<sup>en</sup> $\text{Cp}^{\text{NH}^i\text{Pr}}\text{Fe}(\text{NCMe})(\text{CO})_2$ ]<sup>+</sup> catalysts<sup>107</sup>.** The  $1\text{e}^-$  reduction of complex **22** is followed by stereoselective protonation at the *endo*- $\text{Cp}$  site to give compound **23**, based on density functional theory calculations (other considered protonation sites for this step are highlighted in blue in complex **22**). The *endo*-protonated complex **23** then undergoes ligand-to-metal proton migration after a second reduction event, which enables  $\text{H}_2$  evolution via direct protonation of intermediate **26**. Complexes **24** and **25** are inaccessible on the basis of computed  $\text{pK}_a$  measurements. All redox potentials are referenced to the  $\text{Cp}_2\text{Fe}^{+/0}$  redox couple.  $\text{Cp}$ , cyclopentadienyl;  $\text{Tos}$ , toluenesulfonyl.

a

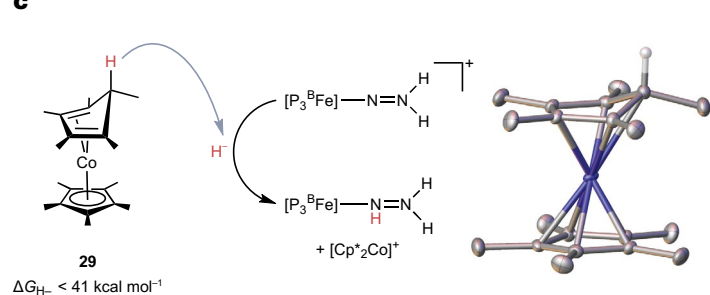


b

Ar-NH <sub>3</sub> <sup>+</sup>	$K_{eq}$ (calc)	$pK_a$ (THF)
	$9 \times 10^5$	3.4
	0.6	6.8
	$2 \times 10^{-3}$	8.6

**Fig. 5 | The role of cyclopentadiene ring activation of decamethylcobaltocene in N<sub>2</sub> reduction catalysis.** **a**, Ring protonation of Cp\*<sub>2</sub>Co gives complex **28**, which has a C–H bond dissociation free energy (BDFE) of 29 kcal mol<sup>-1</sup>, enabling proton-coupled electron transfer reactivity during N<sub>2</sub> reduction catalysis using the boratrane complex [P<sub>3</sub><sup>B</sup>Fe] (ref. 122). **b**,  $pK_a$  dependence on the formation of *exo*-Cp\*Co(*n*<sup>4</sup>-C<sub>5</sub>Me<sub>5</sub>H)<sup>+</sup> (**28**). Increased concentrations of complex **28** in solution

c



enhance N<sub>2</sub> to NH<sub>3</sub> reduction yields with complex [P<sub>3</sub><sup>B</sup>Fe] (refs. 122,124). **c**, The hydricity ( $\Delta G_{H^-}$ ) of complex **29** was determined to be 41 kcal mol<sup>-1</sup>, suggesting that complex **29** (CCDC 1902775) is capable of hydride transfer to a diazenido ligand during N<sub>2</sub> reduction with catalyst [P<sub>3</sub><sup>B</sup>Fe] (ref. 123). Ar, substituted aryl group; Cp\*, pentamethylcyclopentadienyl; Tf, trifluoromethylsulfonate; THF, tetrahydrofuran.

and electron paramagnetic resonance (EPR) experiments revealed that the Cp\* ring of Cp\*<sub>2</sub>Co is protonated in the *exo*-position to generate [(*exo*-*n*<sup>4</sup>-C<sub>5</sub>Me<sub>5</sub>H)CoCp]<sup>+</sup> (**28**), priming it to deliver H<sup>+</sup> via PCET during N<sub>2</sub> reduction catalysed by iron boratrane complex [P<sub>3</sub><sup>B</sup>Fe]<sup>122</sup> (Fig. 5a). The proclivity for C–H bond scission in complex **28** is rationalized by its low bond dissociation free energy (BDFE(CH) < 29 kcal mol<sup>-1</sup>)<sup>123</sup>, driven by re-aromatization of the ring system to the *n*<sup>5</sup>-C<sub>5</sub>Me<sub>5</sub> state and subsequent generation of the diamagnetic [Cp\*<sub>2</sub>Co]<sup>+</sup>. DFT calculations further support this hypothesis by revealing that the calculated N–H bond dissociation enthalpy for an early-stage N<sub>2</sub> reduction intermediate is higher (47 kcal mol<sup>-1</sup>)<sup>122</sup> than the measured C–H bond dissociation enthalpy of complex **28** (< 29 kcal mol<sup>-1</sup>)<sup>123</sup>. Thus, Cp\* ring protonation was proposed to be an essential component of delivering reactive H<sup>+</sup> moieties during N<sub>2</sub>RR.

In a separate report, thorough catalytic studies were undertaken using Cp\*<sub>2</sub>Co, demonstrating a strong correlation between N<sub>2</sub>RR activity, acidity of the exogenous cationic acid and its counteranion<sup>124</sup>. Freeze-quench Mössbauer spectra containing stoichiometric amounts of the acid 2,6-dichloroanilinium trifluoromethanesulfonate ([<sup>2,6</sup>-ClPhNH<sub>3</sub>][OTf]) with the early-stage N<sub>2</sub>-fixed intermediate [P<sub>3</sub><sup>B</sup>Fe-N≡N]<sup>+</sup> did not furnish the known protonation product [P<sub>3</sub><sup>B</sup>Fe-NH<sub>2</sub>]<sup>+</sup> (ref. 125), suggesting that Cp\*<sub>2</sub>Co and acid must react with one another before productive N<sub>2</sub>RR can occur. DFT calculations revealed a correlation between the equilibrium constant ( $K_{eq}$ ) for the formation of complex **28** and the  $pK_a$  of the exogenous acid used<sup>124</sup> (Fig. 4b). In all the three instances, protonation is kinetically facile but stronger acids increase the concentration of available [(*exo*-*n*<sup>4</sup>-C<sub>5</sub>Me<sub>5</sub>H)CoCp]<sup>+</sup> (**28**)

in solution through a computed transition state involving hydrogen-bonded [OTf]<sup>-</sup>. Therefore, the observed  $pK_a$  effects on catalytic activity largely arise from the differences in concentration of protonated metallocene relative to Fe catalyst, with higher concentrations of complex **28** enhancing the rate of N<sub>2</sub>RR. To further show the critical role of metallocene-mediated N<sub>2</sub>RR, cyclic voltammetry (CV) studies with [P<sub>3</sub><sup>B</sup>Fe], exogenous acid and [Cp\*<sub>2</sub>Co]<sup>+</sup> revealed a current enhancement in comparison to CVs without added metallocene. Controlled potential electrolysis experiments with added metallocene also showed a modest increase in overall NH<sub>3</sub> yield, verifying that [P<sub>3</sub><sup>B</sup>Fe] is a bona fide molecular electrocatalyst for the reduction of N<sub>2</sub> to NH<sub>3</sub> in the presence of exogenous acid and a Cp\*<sub>2</sub>Co PCET mediator.

Unequivocal spectroscopic evidence for the formation of complex **28** was later reported, in which both the *endo*-isomers and *exo*-isomers were thoroughly characterized using pulse EPR spectroscopic techniques<sup>123</sup>. Protonating Cp\*<sub>2</sub>Co with a sterically unencumbered strong acid such as HOTf at low temperature generated a 10:1 mixture of *endo*-isomers and *exo*-isomers, with computations revealing the latter being more thermochemically stable by approximately 2 kcal mol<sup>-1</sup>. By choosing a bulkier acid, the *endo*/*exo* ratio can become 3:10, as measured by X-band EPR spectroscopy. On the basis of steric arguments, the *exo*-isomer is the only one considered to be active for PCET. Although the X-ray structure of [(*exo*-*n*<sup>4</sup>-C<sub>5</sub>Me<sub>5</sub>H)CoCp]<sup>+</sup> (**28**) remains elusive, the reduction product (*exo*-*n*<sup>4</sup>-C<sub>5</sub>Me<sub>5</sub>H)CoCp\* (**29**) can be isolated and structurally characterized (Fig. 4c). By using thermochemical free energy relationships, the C–H BDFE and hydride donor ability (hydricity) of complexes **28** and **29** were experimentally determined,

respectively, validating the exceptionally weak C–H BDFE of the radical cation (<29 kcal mol<sup>-1</sup>) and potent hydride donor ability of the neutral adduct (<41 kcal mol<sup>-1</sup>). Therefore, it was posited that complex **29** may also serve as a hydride donor during catalytic N<sub>2</sub>RR, delivering a hydride equivalent to the proximal N atom of a coordinated diazenido ligand.

Although the unique reactivity of Cp<sup>\*</sup>Co has been thoroughly demonstrated through the vignette of N<sub>2</sub>RR catalysed by [P<sub>3</sub>BFe], it is not a general-purpose PCET/hydride donor for N<sub>2</sub>RR. An isostructural silatrane ligand that uses an Si anchor in place of boron is inactive for N<sub>2</sub>RR catalysis under otherwise identical reaction conditions<sup>122</sup>. Recently, Peters and co-workers<sup>126</sup> reported a more generally compatible class of amine-functionalized Cp<sub>2</sub>Co mediators that deliver H<sup>+</sup> via N–H bond cleavage for electrocatalytic N<sub>2</sub>RR. In summary, redox-active metallocene mediators have proven to be successful at delivering potent H<sup>+</sup> to inert substrates such as N<sub>2</sub> via C–H or N–H bond activation pathways.

### Stoichiometric hydrogen atom and hydride transfer reactions

The Fe<sup>III</sup> hydride complex [Cp<sup>\*</sup>Fe(dppe)H]<sup>+</sup> (**30**; 1,2-bis(diphenylphosphino)ethane (dppe)) was isolated in 1992 via oxidation of the neutral 18e<sup>-</sup> complex Cp<sup>\*</sup>Fe(dppe)H using Fe<sup>+</sup> (ref. 127) (Fig. 6). After X-ray structural characterization and analysis via EPR and <sup>57</sup>Fe Mössbauer spectroscopies, a follow-up report reacted complex **30** with CO, which was proposed to generate the formally 19e<sup>-</sup> intermediate [Cp<sup>\*</sup>FeH(dppe)(CO)]<sup>+</sup> (ref. 128). Reduction of [Cp<sup>\*</sup>FeH(dppe)(CO)]<sup>+</sup>

with Cp<sub>2</sub>Co furnishes the stable 18e<sup>-</sup> complex (*endo*-η<sup>4</sup>-C<sub>5</sub>Me<sub>5</sub>H)Fe(dppe)CO (**31**), which was further characterized by <sup>1</sup>H and <sup>31</sup>P NMR spectroscopy. Re-examination of the X-band EPR spectra of the putative [Cp<sup>\*</sup>FeH(dppe)(CO)]<sup>+</sup>, including additional pulse EPR spectroscopic data, determined that the <sup>1</sup>H and <sup>31</sup>P hyperfine parameters differ significantly from terminal transition metal hydrides and the complex is actually [(*endo*-η<sup>4</sup>-C<sub>5</sub>Me<sub>5</sub>H)Fe<sup>l</sup>(dppe)CO]<sup>+</sup> (ref. 129) (**32**) (Fig. 6). This structural assignment was also confirmed by X-ray crystallography. Notably, warming a sample of complex **32** to room temperature under a CO atmosphere yields the complex [Cp<sup>\*</sup>Fe(dppe)CO]<sup>+</sup> (**33**) and releases 0.5 equivalents of H<sub>2</sub> in nearly quantitative yield, suggesting that the C–H BDFE of this paramagnetic ring-activated species is lower than the driving force for homolytic H<sub>2</sub> formation (ΔG°(1/2 H<sub>2</sub> → H<sup>•</sup>) = 52 kcal mol<sup>-1</sup>)<sup>130</sup>. Consistent with this interpretation, thermochemical analysis of complex **32** indicates that the C–H BDFE is less than 36 kcal mol<sup>-1</sup>. Interestingly, complex **31** is able to transfer a hydride to CO<sub>2</sub>, indicating that its hydricity must be less than the hydricity of the formate anion (HCO<sup>-</sup>; approximately 44 kcal mol<sup>-1</sup> in acetonitrile)<sup>13,131</sup>.

The diamagnetic cation **33** was reacted with LiHBET<sub>3</sub> to give the *exo*-isomer (*exo*-η<sup>4</sup>-C<sub>5</sub>Me<sub>5</sub>H)Fe<sup>l</sup>(dppe)CO (**34**), consistent with the selectivity observed for nucleophilic addition reactions on coordinatively saturated complexes described earlier (**1–5**) (Fig. 2). Oxidation of **34** with ferrocenium (Fc<sup>+</sup>) generated the *exo*-substituted radical cation [(*exo*-η<sup>4</sup>-C<sub>5</sub>Me<sub>5</sub>H)Fe<sup>l</sup>(dppe)CO]<sup>+</sup> (**35**), whose low computed BDFE (25 kcal mol<sup>-1</sup>) was also consistent with H<sub>2</sub> release upon warming (Fig. 6).

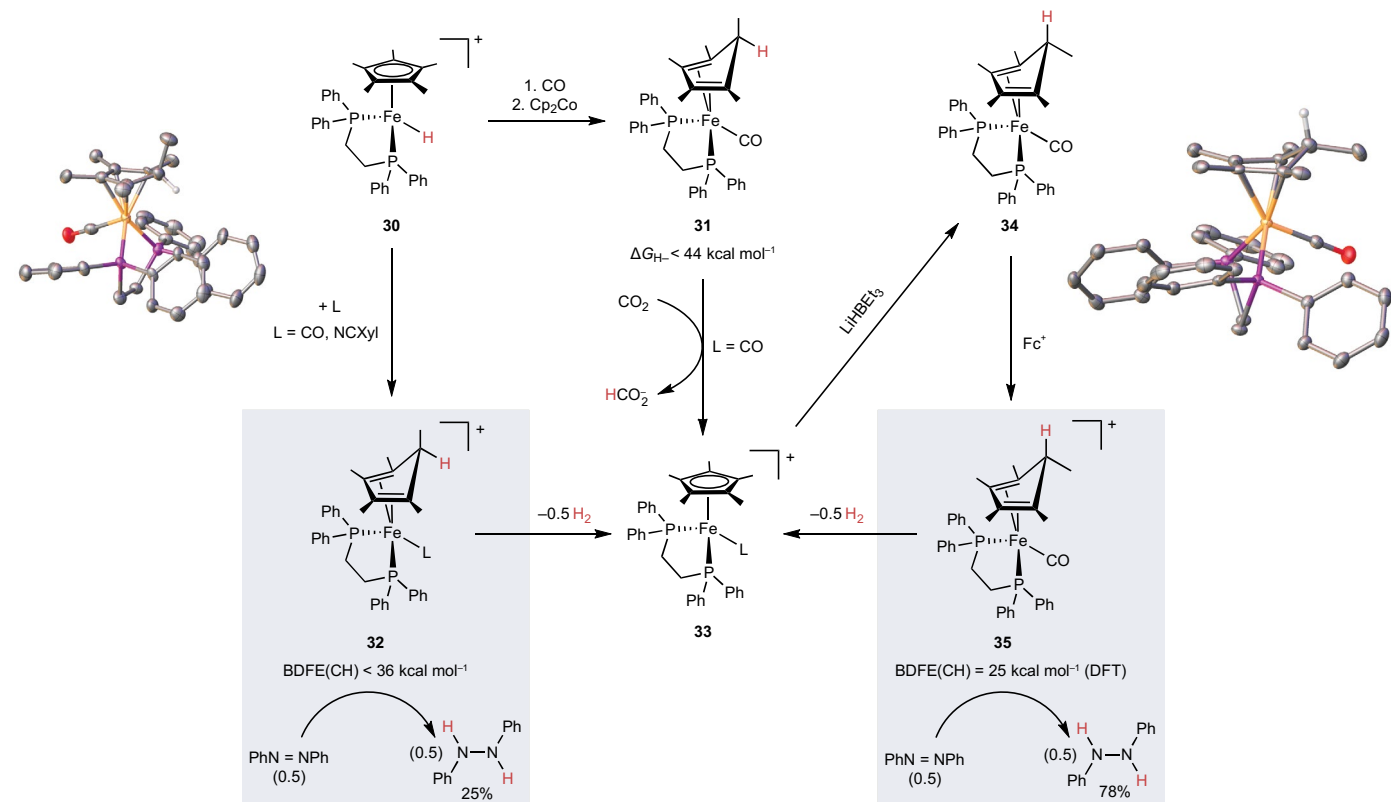


**Fig. 6 | Metal-to-ligand proton migration for generating reactive PCET donors.** Complex **32** (CCDC 1943148; left) releases 0.5 equivalents of H<sub>2</sub> after CO addition to complex **30**. Compound **31** was found to transfer hydride (H<sup>–</sup>) in the presence of CO<sub>2</sub> to generate formate (HCO<sub>2</sub><sup>–</sup>). The *exo*-isomer **34** (CCDC 2021151; right) can also be synthesized via hydride transfer from complex **33**,

and 1e<sup>–</sup> oxidation yields complex **35**. Both **32** and **35** are capable of transferring hydrogen atoms to azobenzene to generate diphenylhydrazine<sup>129</sup>. BDFE, bond dissociation free energy; Cp, cyclopentadienyl; DFT, density functional theory; Fc<sup>+</sup>, ferrocenium; PCET, proton-coupled electron transfer; Xyl, xylyl.

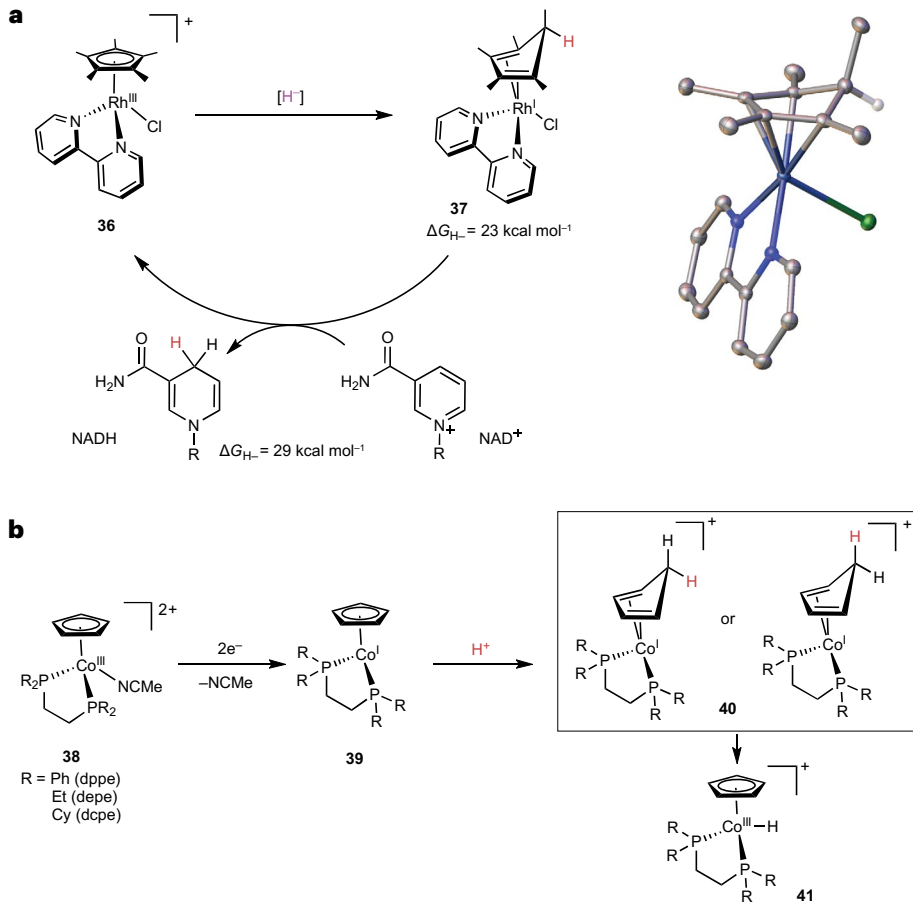


**Fig. 7 | Ring-activated Cp<sup>\*</sup>Rh and CpCo complexes for hydride and proton transfer.**

**a**, Equilibrium measurements determine the thermochemical hydricity ( $\Delta G_{H^-}$ ) of **37** (CCDC 1447440), which favourably transfers H<sup>-</sup> to NAD<sup>+</sup> (ref. 132). **b**, Proposed mechanism involving electrochemical reduction and formation of Co-H complexes via Cp ring protonation of **39** (ref. 134). Cp, cyclopentadienyl; Cp<sup>\*</sup>, pentamethylcyclopentadienyl; dcpe, 1,2-bis(dicyclohexylphosphino)ethane; depe, 1,2-bis(diethylphosphino)ethane; dppe, 1,2-bis(diphenylphosphino)ethane.

To demonstrate the utility of transferring reactive hydrogen atoms to other substrates, exposure of complexes **32** or **35** to azobenzene at  $-78^{\circ}\text{C}$  generated 1,2-diphenylhydrazine (BDFE(N-H)<sub>avg</sub> = 65 kcal mol<sup>-1</sup>) in 25% and 78% yield, respectively (Fig. 6, bottom). The only observable by-products are H<sub>2</sub> and complex **33** and using ring-deuterated Fe analogues ( $\eta^4\text{-C}_5\text{Me}_5\text{D}$ ) resulted in the formation of PhDN-NDPh. Although these systems suffer from thermal instability and deleterious H<sub>2</sub> formation, the incredibly weak C-H bonds of metalloradicals **32** and **35** demonstrated that PCET chemistry is possible with group 8 piano-stool complexes.

In contrast to using H<sup>+</sup> and H<sup>-</sup> transfer for H<sub>2</sub> production and N<sub>2</sub> reduction described in the previous sections, organic and inorganic sources of hydride (H<sup>-</sup>) can also have a key role in catalysis, chemical energy storage and chemical energy conversion<sup>8</sup>. Concurrent with the 2016 discovery that protonation of Cp<sup>\*</sup>Rh<sup>I</sup>(bpy) (**15**) generated (*endo*- $\eta^4\text{-C}_5\text{Me}_5\text{H}$ )Rh<sup>I</sup>Br(bpy) (**16**), Miller and co-workers<sup>132</sup> reported the preparation and structural elucidation of (*endo*- $\eta^4\text{-C}_5\text{Me}_5\text{H}$ )Rh<sup>I</sup>Cl(bpy) (**37**) via two different synthetic pathways starting from [Cp<sup>\*</sup>Rh<sup>III</sup>Cl(bpy)]<sup>+</sup> (**36**) (Fig. 7a). The aqueous hydricity of complex **37** was found to be 23 kcal mol<sup>-1</sup>, enabling stoichiometric hydride transfer to the enzyme cofactor NAD<sup>+</sup> ( $\Delta G_{H^-} = 29 \text{ kcal mol}^{-1}$ ), regenerating complex **36** and producing 1,4-NADH. Thus, direct hydride transfer from an *endo*- $\eta^4\text{-C}_5\text{Me}_5\text{H}$  moiety is possible on thermochemical grounds in bio-organometallic 1,4-NADH regeneration catalysis. However, recent DFT calculations on hydride transfer from [ex*o*-( $\eta^4\text{-C}_5\text{Me}_5\text{H}$ )Rh<sup>I</sup>(bpy)]<sup>+</sup>

(**17**) (Fig. 3) to NAD<sup>+</sup> suggest that direct H<sup>-</sup> transfer from the CpH ring is kinetically disfavoured over H<sup>-</sup> transfer from the transition metal hydride complex (**18**)<sup>133</sup>.

### Stoichiometric proton-coupled electron transfer reactions

In general, transition metal hydride intermediates are frequently observed and/or proposed in chemical energy conversion reactions involving H<sub>2</sub> and CO<sub>2</sub>. As demonstrated through piano-stool Fe complexes (Figs. 4, 6), PCET processes containing Cp ligands can involve the interconversion of  $\eta^4\text{-C}_5\text{Me}_5\text{H}$  moieties and metal hydride intermediates. To better understand the relationship between the kinetics of Co-H formation and the strength of exogenous acid in [CpCo(dxpe)]<sup>2+</sup> (**38**; dxpe = dppe, depe, dcpe), Dempsey and co-workers investigated the proton transfer kinetics under an applied cathodic bias via CV<sup>134</sup> (Fig. 7b). The coordinated acetonitrile ligand dissociated after 2e<sup>-</sup> reduction and in the presence of acid, the CoH complex **41** is generated. To probe this mechanism further, the 2e<sup>-</sup> reduction product Co<sup>I</sup>Cp(dppe) (**39**) was reacted with weak and strong deuterated acids, and deuterium incorporation is observed at both the Cp ring and CoH positions of complex **41**. Therefore, deuteration of the Cp ring likely occurs through *endo*-protonation or *exo*-protonation to generate complex **40** before formation of complex **41**. Ground-state computational data indicate that initial Cp ligand protonation followed by ligand-to-metal proton migration are exothermic ( $\Delta G^{\circ} \approx -20 \text{ kcal mol}^{-1}$ ), strongly disfavouring metal-ligand

tautomerization equilibria. Thus, protonation may be indiscriminate to *exo* versus *endo* attack, which would support the observed CoD/CpD isotope distribution (Fig. 7b). These data also suggest that there is a substantially larger kinetic barrier for direct protonation of the metal centre, contrasting with the kinetically preferred direct metal protonation pathway for Rh complex **18** described earlier<sup>95</sup>. Nonetheless, a seemingly ‘simple’ PCET reaction with an Earth-abundant metal proceeds through a series of unexpected elementary reaction steps involving Cp ring activation.

## Conclusions and future outlook

The Cp ligand is a ubiquitous ancillary ligand in transition metal chemistry. In certain cases, however, the contiguous carbon ring is susceptible to attack by nucleophiles, electrophiles or radicals. Addition of such functional groups can occur in the *exo*-position or *endo*-position relative to the metal centre and breaks the aromaticity of the  $\eta^5$ -Cp ring, generating an  $\eta^4$ -diene ( $\eta^4$ -CpH) ligand coordinated to a transition metal. Although largely considered a laboratory curiosity in the decades following the discovery of ferrocene, developments since 2016 have revealed that the chemically non-innocent character of Cp, Cp\* and other Cp derivatives can be essential to the electrocatalytic reduction of H<sup>+</sup> to H<sub>2</sub>, catalytic PCET of H<sup>+</sup> to N<sub>2</sub> and transfer of H<sup>+</sup>/H<sup>-</sup> to organic substrates. Carbon–hydrogen bond strength analyses via experiment and/or computation have emerged as indispensable tools to rationalize H<sup>+</sup>, H<sup>·</sup> and H<sup>-</sup> movement with ring-activated complexes, enabling the measurement of C–H acidity, BDFE and hydricity, respectively. Thus, the phenomenon of Cp ring activation is more general than initially thought, and practitioners are encouraged to (re)consider pathways involving ring activation of Cp ligands, especially when proton, hydrogen atom or hydride transfer is invoked to rationalize reaction outcomes.

Ground-state thermochemical measurements have allowed researchers to rationally design Cp/CpH-mediated catalysts with a sufficient driving force for sustainable fuel-forming reactions; however, these results do not provide kinetic information for the making and breaking of ligand-based C–H bonds. It has been recently suggested that slow Cp ring protonation with Cp<sub>2</sub>Co is governed by the high ligand reorganization energy associated with a change from  $sp^2$  to  $sp^3$  hybridization upon addition of H<sup>+</sup> (ref. 135). Although this may be true for Cp<sub>2</sub>Co, a key challenge moving forward in this field will be to understand the requirements for promoting rapid H<sup>+</sup>/H<sup>·</sup>/H<sup>-</sup> transfer via Cp ring activation by exploring variations in metal centre (precious versus Earth abundant), overall spin state (paired versus unpaired electrons), ancillary ligand environment (metallocene versus piano-stool structure) and Cp ligand substitution pattern (Cp, Cp\* and other derivatives). Another key challenge for expanding the vistas of ring-activated CpH complexes will be to avoid H<sub>2</sub> production via homolytic or heterolytic H–H bond formation pathways when the highly reactive H<sup>+</sup>/H<sup>·</sup> moiety is intended for delivery to other substrates of interest. Overcoming these challenges, among others, will be achieved by surveying kinetic and thermodynamic landscapes for the myriad of other Cp-containing complexes awaiting deeper exploration.

Published online: 31 May 2023

## References

- Chirik, P. J. Group 4 transition metal sandwich complexes: still fresh after almost 60 years. *Organometallics* **29**, 1500–1517 (2010).
- Field, L. D., Lindall, C. M., Masters, A. F. & Clentsmith, G. K. B. Penta-arylcyclopentadienyl complexes. *Coord. Chem. Rev.* **255**, 1733–1790 (2011).
- Mas-Rosello, J., Herranz, A. G., Audic, B., Laverny, A. & Cramer, N. Chiral cyclopentadienyl ligands: design, syntheses, and applications in asymmetric catalysis. *Angew. Chem. Int. Ed.* **60**, 13198–13224 (2021).
- Shapiro, P. J. The evolution of the ansa-bridge and its effect on the scope of metallocene chemistry. *Coord. Chem. Rev.* **231**, 67–81 (2002).
- Enders, M. & Baker, W. R. Synthesis of aryl- and heteroaryl-substituted cyclopentadienes and indenes and their use in transition metal chemistry. *Curr. Org. Chem.* **10**, 937–953 (2006).
- Morris, R. H. Brønsted–Lowry acid strength of metal hydride and dihydrogen complexes. *Chem. Rev.* **116**, 8588–8654 (2016).
- Shevick, S. L. et al. Catalytic hydrogen atom transfer to alkenes: a roadmap for metal hydrides and radicals. *Chem. Sci.* **11**, 12401–12422 (2020).
- Wiedner, E. S. et al. Thermodynamic hydricity of transition metal hydrides. *Chem. Rev.* **116**, 8655–8692 (2016).
- Wiedner, E. S., Appel, A. M., Raugei, S., Shaw, W. J. & Bullock, R. M. Molecular catalysts with diphosphine ligands containing pendant amines. *Chem. Rev.* **122**, 12427–12474 (2022).
- Kuo, J. L., Lorenc, C., Abuyuan, J. M. & Norton, J. R. Catalysis of radical cyclizations from alkyl iodides under H<sub>2</sub>: evidence for electron transfer from [CpV(CO)<sub>3</sub>H]<sup>+</sup>. *J. Am. Chem. Soc.* **140**, 4512–4516 (2018).
- Kuo, J. L. et al. Thermodynamics of H<sup>+</sup>/H<sup>·</sup>/H<sup>-</sup>/e<sup>-</sup> transfer from [CpV(CO)<sub>3</sub>H]<sup>+</sup>: comparisons to the isoelectronic CpCr(CO)<sub>3</sub>H. *Organometallics* **38**, 4319–4328 (2019).
- Yao, C., Dahmen, T., Gansäuer, A. & Norton, J. Anti-Markovnikov alcoholos via epoxide hydrogenation through cooperative catalysis. *Science* **364**, 764–767 (2019).
- DuBois, D. L. & Berning, D. E. Hydricity of transition-metal hydrides and its role in CO<sub>2</sub> reduction. *Appl. Organomet. Chem.* **14**, 860–862 (2000).
- Walddie, K. M., Ostericher, A. L., Reineke, M. H., Sasayama, A. F. & Kubiak, C. P. Hydricity of transition-metal hydrides: thermodynamic considerations for CO<sub>2</sub> reduction. *ACS Catal.* **8**, 1313–1324 (2018).
- Barlow, J. M. & Yang, J. Y. Thermodynamic considerations for optimizing selective CO<sub>2</sub> reduction by molecular catalysts. *ACS Cent. Sci.* **5**, 580–588 (2019).
- Macomber, D. W., Hart, W. P. & Rausch, M. D. *Advances in Organometallic Chemistry* Vol. 21 (eds Stone, F. G. A. & West, R.) 1–55 (Academic, 1982).
- Green, M. L. H., Pratt, L. & Wilkinson, G. 760. A new type of transition metal–cyclopentadiene compound. *J. Chem. Soc.* **1959**, 3753–3767 (1959).  
**The first characterization of Cp ring activation products with nucleophilic and radical reagents.**
- Fischer, E. O. & Herberich, G. E. Über aromatenkomplexe von metallen, XLIV. Über die reaktivität des di-cyclopentadienyl-kobalt(III)-kations. *Chem. Ber.* **94**, 1517–1523 (1961).
- Churchill, M. R., Mason, R. & Nyholm, R. S. The crystal and molecular structure of  $\pi$ -cyclopentadienyl-1-phenylcyclopentadiene cobalt. *Proc. Math. Phys. Eng.* **279**, 191–209 (1964).
- Lehmkühl, H. & Nehl, H. F. Über (cyclopentadienyl)organylcobalt-komplexe. *Chem. Ber.* **117**, 3443–3456 (2006).
- Davison, A., Green, M. L. H. & Wilkinson, G. 620.  $\pi$ -Cyclopentadienyl- and cyclopentadiene-iron carbonyl complexes. *J. Chem. Soc. Dalton Trans.* **1961**, 3172–3177 (1961).
- Angelici, R. J. & Fischer, E. O. New cyclopentadienyl complexes of rhodium. *J. Am. Chem. Soc.* **85**, 3733–3735 (1963).
- Davies, S. G., Green, M. L. H. & Mingos, D. M. P. Nucleophilic addition to organotransition metal cations containing unsaturated hydrocarbon ligands: a survey and interpretation. *Tetrahedron* **34**, 3047–3077 (1978).
- Yan, Y., Zhang, J., Qiao, Y. & Tang, C. Facile preparation of cobaltocenium-containing polyelectrolyte via click chemistry and RAFT polymerization. *Macromol. Rapid Commun.* **35**, 254–259 (2014).
- Yan, Y., Zhang, J., Wilbon, P., Qiao, Y. & Tang, C. Ring-opening metathesis polymerization of 18-e<sup>-</sup> cobalt(I)-containing norbornene and application as heterogeneous macromolecular catalyst in atom transfer radical polymerization. *Macromol. Rapid Commun.* **35**, 1840–1845 (2014).
- Enders, M., Kohl, G. & Pritzkow, H. Synthesis of main group and transition metal complexes with the (8-quinolyl)cyclopentadienyl ligand and their application in the polymerization of ethylene. *Organometallics* **23**, 3832–3839 (2004).
- Yan, Y. et al. Syntheses of monosubstituted rhodocenium derivatives, monomers, and polymers. *Macromolecules* **48**, 1644–1650 (2015).
- Vanicek, S. et al. Chemoselective, practical synthesis of cobaltocenium carboxylic acid hexafluorophosphate. *Organometallics* **33**, 1152–1156 (2014).
- Pita-Milleiro, A. et al. Unveiling the latent reactivity of Cp\* ligands (C<sub>5</sub>Me<sub>5</sub><sup>\*</sup>) toward carbon nucleophiles on an iridium complex. *Inorg. Chem.* **62**, 5961–5971 (2023).
- Broadhead, G. D., Osgerby, J. M. & Pauson, P. L. Ferrocene derivatives. Part V: Ferrocenealdehyde. *J. Chem. Soc.* **1958**, 650–656 (1958).
- Rosenblum, M., Santer, J. O. & Howells, W. G. The chemistry and structure of ferrocene. VIII: Interannular resonance and the mechanism of electrophilic substitution. *J. Am. Chem. Soc.* **85**, 1450–1458 (1963).
- Pauson, P. L. in *Encyclopedia of Reagents for Organic Synthesis* (Wiley, 2001).
- Malischewski, M. et al. Protonation of ferrocene: a low-temperature X-ray diffraction study of [Cp<sub>2</sub>FeH]<sup>+</sup>(PF<sub>6</sub>) reveals an iron-bound hydrido ligand. *Angew. Chem. Int. Ed.* **56**, 13372–13376 (2017).

34. Court, T. L. & Werner, H. Studies on the reactivity of metal  $\pi$ -complexes. *J. Organomet. Chem.* **65**, 245–251 (1974).

35. El Murr, N. & Lavorin, E. Electrochimie de composés organométalliques. I. Electrosynthèse de cyclopentadiène cyclopentadiényl cobalt substitués. *Can. J. Chem.* **54**, 3350–3356 (1976).

36. El Murr, N. & Lavorin, E. Syntheses using electrochemically generated cobaltocene or cobaltocene anion. *Tetrahedr. Lett.* **16**, 875–878 (1975).

37. Koelle, U. & Khouzami, F. Permethylated electron-excess metallocenes. *Angew. Chem. Int. Ed. Engl.* **19**, 640–641 (1980).

38. Werner, H. & Dernberger, T. Untersuchungen zur reaktivität von metall- $\pi$ -komplexen. *J. Organomet. Chem.* **198**, 97–103 (1980).

39. Wilkinson, G., Cotton, F. A. & Birmingham, J. M. On manganese cyclopentadienide and some chemical reactions of neutral bis-cyclopentadienyl metal compounds. *J. Inorg. Nucl. Chem.* **2**, 95–113 (1956).

40. Katz, S., Weiler, J. F. & Voigt, A. F. Reaction of biscyclopentadienylcobalt(II) with organic halides. *J. Am. Chem. Soc.* **80**, 6459 (1958).

41. Herberich, G. E., Bauer, E. & Schwarzer, J. Untersuchungen zur reaktivität organometallischer komplexe III. Über die reaktion von dicyclopentadienylkobalt mit halogenmethanen. *J. Organomet. Chem.* **17**, 445–452 (1969).

42. Herberich, G. E. & Schwarzer, J. Free radical additions to dicyclopentadienylcobalt. *Angew. Chem. Int. Ed. Engl.* **9**, 897–897 (1970).

**Strong mechanistic evidence for radical-based Cp ring activation.**

43. Herberich, G. E. & Schwarzer, J. Untersuchungen zur reaktivität organometallischer komplexe. *J. Organomet. Chem.* **34**, C43–C47 (1972).

44. Herberich, G. E., Carstensen, T., Klein, W. & Schmidt, M. U. Reaction of 19-valence-electron sandwich complexes with alkyl-halides — a radical-clock investigation. *Organometallics* **12**, 1439–1441 (1993).

45. Gusev, O. V. et al. Synthesis of  $\eta^5$ -1,2,3,4,5-pentamethylcyclopentadienyl-platinum complexes. *J. Organomet. Chem.* **472**, 359–363 (1994).

46. Gusev, O. V. et al. Bis( $\eta^5$ -pentamethylcyclopentadienyl)-and( $\eta^5$ -cyclopentadienyl) ( $\eta^5$ -pentamethylcyclopentadienyl)-platinum dication: Pt(IV) metallocenes. *J. Organomet. Chem.* **480**, c16–c17 (1994).

47. Jernakoff, P., Fox, J. R. & Cooper, N. J. Electrophilic addition of  $\text{CCl}_4$  to a cyclopentadienyl ligand in the tungstenocene carbonyl [ $W(\eta^5\text{-C}_5\text{H}_5)_2(\text{CO})$ ] to give [ $W(\eta^5\text{-C}_5\text{H}_5)(\eta^4\text{-C}_5\text{H}_5\text{-exo-CCl}_3)(\text{CO})_2$ ]. *J. Organomet. Chem.* **512**, 175–181 (1996).

48. O'Connor, J. M. & Casey, C. P. Ring-slippage chemistry of transition metal cyclopentadienyl and indenyl complexes. *Chem. Rev.* **87**, 307–318 (2002).

49. Suvorova, O. N. et al. Reactions of metallocenes during intercalation into the layered  $\text{TiSe}_2$  lattice. *Russ. Chem. Bull.* **56**, 910–914 (2007).

50. Tsai, W. M., Rausch, M. D. & Rogers, R. D. Improved synthesis of pentabenzylcyclopentadiene and study of the reaction between pentabenzylcyclopentadiene and iron pentacarbonyl. *Organometallics* **15**, 2591–2594 (1996).

51. Donovan, B. T., Hughes, R. P., Kowalski, A. S., Trujillo, H. A. & Rheingold, A. L. Stereoselective rhodium-promoted ring closure of an  $\eta^4$ -1,3-pentadienyl ligand to an  $\eta^4$ -1,3-cyclopentadiene, with subsequent regiospecific *endo*-H migration: molecular structure of  $[\text{Rh}(\eta^5\text{-C}_5\text{H}_5)(1\text{-}4\text{-}R)\text{-C}_5\text{H}_3\text{-}1,2\text{-exo-5'\text{-}Bu}_3]$ . *Organometallics* **12**, 1038–1043 (2002).

52. Busetto, L., Marchetti, F., Zucchini, S. & Zanotti, V. Addition of isocyanides at Diiron  $\mu$ -vinyliminium complexes: synthesis of novel ketenimine-bis(alkylidene) complexes. *Organometallics* **27**, 5058–5066 (2008).

53. Bullock, R. M., Headford, C. E. L., Hennessy, K. M., Kegley, S. E. & Norton, J. R. Intramolecular hydrogen exchange among the coordinated methane fragments of  $\text{Cp}_2\text{W}(\text{H})\text{CH}_3$ : evidence for the formation of a  $\sigma$  complex of methane prior to elimination. *J. Am. Chem. Soc.* **111**, 3897–3908 (1989).

54. Cadenbach, T., Gernel, C., Schmid, R. & Fischer, R. A. Mechanistic insights into an unprecedented C-C bond activation on a Rh/Ga bimetallic complex: a combined experimental/computational approach. *J. Am. Chem. Soc.* **127**, 17068–17078 (2005).

55. Cooper, R. L., Green, M. L. H. & Moelwyn-Hughes, J. T. Studies on the dicyclopentadienyl hydrides of rhodium and tungsten. *J. Organomet. Chem.* **3**, 261–268 (1965).

56. Davidson, J. L., Green, M., Stone, F. G. A. & Welch, A. J. Syntheses involving co-ordinatively unsaturated cyclopentadienyl-molybdenum and -tungsten complexes: molecular and crystal structure of  $[\text{Mo-C}(\text{CF}_3)_2\text{C}(\text{CF}_3)\text{C}_5\text{H}_5\text{H}_5(\text{CF}_3\text{C}_2\text{CF}_3)(\eta^5\text{-C}_5\text{H}_5)]$ . *J. Chem. Soc. Dalton Trans.* **3**, 287–294 (1977).

57. Gusev, O. V. et al. Electrochemical generation of 19- and 20-electron rhodocenium complexes and their properties. *J. Organomet. Chem.* **452**, 219–222 (1993).

58. Davidson, J. L., Green, M., Stone, F. G. A. & Welch, A. J. Insertion reactions of hexafluorobut-2-yne, tetrafluoroethylene, and hexafluoroacetone with  $\eta^5$ -cyclopentadienyl-iron, -ruthenium, -palladium, and -molybdenum complexes: molecular and crystal structures of  $[\text{Fe}_2(\text{CO})_4(\text{C}_4\text{F}_7)_2\text{CO}](\eta^5\text{-C}_5\text{H}_5)_2$  and  $[\text{Fe}(\text{COCF}_2\text{C}_5\text{H}_5)(\eta^5\text{-C}_5\text{H}_5)]$ . *J. Chem. Soc. Dalton Trans.* **20**, 2044–2053 (1976).

59. Carpenter, N. E., Khan, M. A. & Nicholas, K. M. Selective metal-to-ring alkyl migration during irradiation of  $\text{CpFe}(\text{CO})_2\text{CHPh}(\text{OSiMe}_3)$ . *Organometallics* **18**, 1569–1570 (1999).

60. Jones, W. D. & Maguire, J. A. Preparation and reaction dynamics of ( $\eta^4\text{-C}_5\text{H}_5\text{)}\text{Re}(\text{PPh}_3)_2\text{H}_5$  a structurally characterized  $\eta^4$ -cyclopentadiene complex. *Organometallics* **4**, 951–953 (1985).

61. Rupp, R. et al.  $^4$ -Coordination of dienes and heterodienes to the tripodCobalt(II) template  $[\text{CH}_3\text{C}(\text{CH}_2\text{PPh}_3)_2\text{Co}]^+$ : synthesis, structure, and dynamics. *Eur. J. Inorg. Chem.* **2000**, 523–536 (2000).

62. Enders, M. et al. Coordination chemistry of neutral quinolyl- and aminophenylcyclopentadiene derivatives. *J. Organomet. Chem.* **641**, 81–89 (2002).

63. Macias, R. et al. Effects of metal-centre orbital control on cluster character and electron distribution between borane and hydrocarbon ligands; significance of the structures of  $[\mu\text{-9,10-(SMe)-8,8-(PPh}_3)_2\text{-nido-8,7-}(\text{RhSB}_3\text{H}_3)]$  and  $[\mu\text{-9,10-(SMe)-8-(n}^4\text{-C}_5\text{Me}_5\text{H)-nido-8,7-}(\text{RhSB}_3\text{H}_3)]$ . *J. Chem. Soc. Dalton Trans.* **2**, 149–152 (1997).

64. Hitchcock, P. B., Nixon, J. F. & Buyukkidan, N. S. Remarkable organophosphorus cage compounds from the reaction of cobaltocene and the triphosphole  $\text{P}_3\text{C}_2\text{Bu}^2\text{CH}(\text{SiMe}_3)_2$ : crystal and molecular structures of  $[\text{Co}(\eta^5\text{-C}_5\text{H}_5)(\eta^4\text{-C}_4\text{H}_4\text{CHCHP}_2\text{C}_4\text{Bu}^2)]$  and  $\text{P}_2\text{C}_4\text{Bu}^4\text{CH}(\text{SiMe}_3)$ . *Chem. Commun.* **24**, 2720–2721 (2001).

65. Nishihara, Y., Deck, K. J., Shang, M. & Fehlner, T. P. Cluster chemistry driven by ligand bulk. Significance of the synthesis of nido-1-( $\eta^5\text{-C}_5\text{Me}_5\text{)}\text{Co}-2-( $\eta^4\text{-C}_5\text{Me}_5\text{H})\text{CoB}_3\text{H}_6$  and its dehydrogenation to nido-2,4- $\{(\eta^5\text{-C}_5\text{Me}_5\text{)}\text{Co}\}_2\text{B}_3\text{H}_7$ . *J. Am. Chem. Soc.* **115**, 12224–12225 (2002).$

66. Nishihara, Y. et al. Synthesis of cobaltaborane clusters from  $[\text{Cp}^*\text{CoCl}_2]$  and monoboranes: new structures and mechanistic implications. *Organometallics* **13**, 4510–4522 (2002).

67. Hodson, B. E., McGrath, T. D. & Stone, F. G. Synthesis, structure, and dynamics of nickelcarboranes incorporating the [nido-7,9- $\text{C}_2\text{B}_9\text{H}_{11}]^2$  ligand. *Inorg. Chem.* **43**, 3090–3097 (2004).

68. Kefalidis, C. E. et al. Can a pentamethylcyclopentadienyl ligand act as a proton-relay in f-element chemistry? Insights from a joint experimental/theoretical study. *Dalton Trans.* **44**, 2575–2587 (2015).

69. Jones, W. D., Kuykendall, V. L. & Selmeczy, A. D. Ring migration reactions of  $(\text{C}_5\text{Me}_5)_2\text{Rh}(\text{PMe}_3)\text{H}_2$  — evidence for  $\eta^3$  slippage and metal-to-ring hydride migration. *Organometallics* **10**, 1577–1586 (1991).

70. Jones, W. D., Rosini, G. P. & Maguire, J. A. Photochemical C–H activation and ligand exchange reactions of  $\text{CpRe}(\text{PPh}_3)_2\text{H}_2$ : phosphine dissociation is not involved. *Organometallics* **18**, 1754–1760 (1999).

71. Reger, D. L., Belmore, K. A., Atwood, J. L. & Hunter, W. E. The *cis* addition of hydride to  $\eta^2$ -alkyne complexes by initial reaction at an  $\eta^5$ -cyclopentadienyl ( $\eta^5\text{-C}_5\text{H}_5$ ) ring: crystal and molecular structure of the carbonyl- $\eta^5$ -cyclopentadienyliron complex ( $\eta^5\text{-C}_5\text{H}_5\text{)}\text{FeCO}(\text{PPh}_3)[\eta^1\text{-}(\text{E})\text{-C}(\text{CO}_2\text{Et})=\text{C}(\text{H})\text{Me}]$ . *J. Am. Chem. Soc.* **105**, 5710–5711 (2002).

72. Gleiter, R., Bleiholder, C. & Rominger, F.  $\sigma$ -Metallocenylmethylium ions and isoelectronic fulvene complexes of  $d^6$  to  $d^9$  metals: structural considerations. *Organometallics* **26**, 4850–4859 (2007).

73. Preethayam, P. et al. Recent advances in the chemistry of pentafulvenes. *Chem. Rev.* **117**, 3930–3989 (2017).

74. Kreindlin, A. Z. & Rybinskaya, M. I. Cationic and neutral transition metal complexes with a tetramethylfulvene or trimethylallyldiene ligand. *Russ. Chem. Rev.* **73**, 417 (2004).

75. Astruc, D. Electron and proton reservoir complexes: thermodynamic basis for C–H activation and applications in redox and dendrimer chemistry. *Acc. Chem. Res.* **33**, 287–298 (2000).

76. Chen, J. G. et al. Beyond fossil fuel-driven nitrogen transformations. *Science* **360**, 6391 (2018).

77. Agarwal, R. G. et al. Free energies of proton-coupled electron transfer reagents and their applications. *Chem. Rev.* **122**, 1–49 (2022).

78. Lewis, N. S. & Nocera, D. G. Powering the planet: chemical challenges in solar energy utilization. *Proc. Natl. Acad. Sci. USA* **103**, 15729–15735 (2006).

79. Rauchfuss, T. B. Diiron azadithiolates as models for the [FeFe]-hydrogenase active site and paradigm for the role of the second coordination sphere. *Acc. Chem. Res.* **48**, 2107–2116 (2015).

80. Lubitz, W., Ogata, H., Rudiger, O. & Reijerse, E. Hydrogenases. *Chem. Rev.* **114**, 4081–4148 (2014).

81. Klug, C. M., Cardenas, A. J. P., Bullock, R. M., O'Hagan, M. & Wiedner, E. S. Reversing the tradeoff between rate and overpotential in molecular electrocatalysts for  $\text{H}_2$  production. *ACS Catal.* **8**, 3286–3296 (2018).

82. Ruppert, R., Herrmann, S. & Steckhan, E. Efficient indirect electrochemical in-situ regeneration of NADH: electrochemically driven enzymatic reduction of pyruvate catalyzed by d-lidh. *Tetrahedr. Lett.* **28**, 6583–6586 (1987).

83. Steckhan, E. et al. Analytical study of a series of substituted (2,2'-bipyridyl) (pentamethylcyclopentadienyl)rhodium and iridium complexes with regard to their effectiveness as redox catalysts for the indirect electrochemical and chemical-reduction of  $\text{NAD}(\text{P})^+$ . *Organometallics* **10**, 1568–1577 (1991).

84. Lo, H. C. et al. Bioorganometallic chemistry. 13. Regioselective reduction of  $\text{NAD}(\text{P})^+$  models, 1-benzylnicotinamide triflate and beta-nicotinamide ribose-5'-methyl phosphate, with in situ generated  $[\text{CpRh}(\text{Bpy})\text{H}]^+$ : structure–activity relationships, kinetics, and mechanistic aspects in the formation of the 1,4-NADH derivatives. *Inorg. Chem.* **40**, 6705–6716 (2001).

85. Ruppert, R., Herrmann, S. & Steckhan, E. Very efficient reduction of  $\text{NAD}(\text{P})^+$  with formate catalyzed by cationic rhodium complexes. *J. Chem. Soc. Chem. Commun.* **17**, 1150–1151 (1988).

86. Fukuzumi, S., Kobayashi, T. & Suenobu, T. Efficient catalytic decomposition of formic acid for the selective generation of  $\text{H}_2$  and  $\text{H}_2\text{O}$  exchange with a water-soluble rhodium complex in aqueous solution. *ChemSusChem* **1**, 827–834 (2008).

87. Kölle, U. & Grätzel, M. Organometallic rhodium(III) complexes as catalysts for the photoreduction of protons to hydrogen on colloidal  $\text{TiO}_2$ . *Angew. Chem. Int. Ed. Engl.* **26**, 567–570 (1987).

88. Cosnier, S., Deronzier, A. & Vlachopoulos, N. Carbon/poly{pyrrole- $[(\text{C}_5\text{Me}_5)_2\text{Rh}^{III}(\text{bpy})\text{Cl}]}$ } modified electrodes: a molecularly-based material for hydrogen evolution ( $\text{bpy} = 2,2'$ -bipyridine). *J. Chem. Soc. Chem. Commun.* **17**, 1259–1261 (1989).

89. Kölle, U., Kang, B. S., Infelta, P., Comte, P. & Grätzel, M. Elektrochemische und pulsradiolytische Reduktion von (pentamethylcyclopentadienyl)(polypyridyl)rhodium-Komplexen. *Chem. Ber.* **122**, 1869–1880 (1989).

90. Blakemore, J. D. et al. Pentamethylcyclopentadienyl rhodium complexes. *Polyhedron* **84**, 14–18 (2014).

91. Quintana, L. M. et al. Proton-hydride tautomerism in hydrogen evolution catalysis. *Proc. Natl Acad. Sci. USA* **113**, 6409–6414 (2016).

**Structural and spectroscopic evidence of metal-to-ligand tautomerism with  $\text{Cp}^*$  ligands and their relevance to  $\text{H}_2$  production.**

92. Kolthoff, I. M., Chantoon, M. K. & Bhowmik, S. Acid-base indicator constants in acetonitrile. *Anal. Chem.* **39**, 315–320 (1967).

93. Appel, A. M. & Helm, M. L. Determining the overpotential for a molecular electrocatalyst. *ACS Catal.* **4**, 630–633 (2014).

94. Kaljurand, I. I. et al. Extension of the self-consistent spectrophotometric basicity scale in acetonitrile to a full span of 28 pKa units: unification of different basicity scales. *J. Org. Chem.* **70**, 1019–1028 (2005).

95. Johnson, S. I., Gray, H. B., Blakemore, J. D. & Goddard, W. A. III Role of ligand protonation in dihydrogen evolution from a pentamethylcyclopentadienyl rhodium catalyst. *Inorg. Chem.* **56**, 11375–11386 (2017).

96. Peng, Y., Ramos-Garcés, M. V., Lionetti, D. & Blakemore, J. D. Structural and electrochemical consequences of  $[\text{Cp}^*]$  ligand protonation. *Inorg. Chem.* **56**, 10824–10831 (2017).

97. Henke, W. C. et al. Ligand substituents govern the efficiency and mechanistic path of hydrogen production with  $[\text{Cp}^*\text{Rh}]$  catalysts. *ChemSusChem* **10**, 4589–4598 (2017).

98. Bullock, R. M. et al. Using nature's blueprint to expand catalysis with Earth-abundant metals. *Science* **369**, 6505 (2020).

99. Liu, T. B., DuBois, D. L. & Bullock, R. M. An iron complex with pendent amines as a molecular electrocatalyst for oxidation of hydrogen. *Nat. Chem.* **5**, 228–233 (2013).

100. Agarwal, T. & Kaur-Ghumaan, S. HER catalysed by iron complexes without a  $\text{Fe}_2\text{S}_2$  core: a review. *Coord. Chem. Rev.* **397**, 188–219 (2019).

101. Artero, V. & Fontecave, M. Hydrogen evolution catalyzed by  $\{\text{CpFe}(\text{CO})_2\}$ -based complexes. *C. R. Chim.* **11**, 926–931 (2008).

102. Darmon, J. M. et al. Iron complexes for the electrocatalytic oxidation of hydrogen: tuning primary and secondary coordination spheres. *ACS Catal.* **4**, 1246–1260 (2014).

103. Brazzolotto, D. et al. Nickel-centred proton reduction catalysis in a model of  $[\text{NiFe}]$  hydrogenase. *Nat. Chem.* **8**, 1054–1060 (2016).

104. Hemming, E. B. et al.  $[\text{Fe}(\text{C}_5\text{Ar}_5)(\text{CO})_2\text{Br}]$  complexes as hydrogenase mimics for the catalytic hydrogen evolution reaction. *Appl. Catal. B* **223**, 234–241 (2018).

105. Helm, M. L., Stewart, M. P., Bullock, R. M., DuBois, M. R. & DuBois, D. L. A synthetic nickel electrocatalyst with a turnover frequency above 100,000  $\text{s}^{-1}$  for  $\text{H}_2$  production. *Science* **333**, 863–866 (2011).

106. Carroll, M. E., Barton, B. E., Rauchfuss, T. B. & Carroll, P. J. Synthetic models for the active site of the  $[\text{FeFe}]$ -hydrogenase: catalytic proton reduction and the structure of the doubly protonated intermediate. *J. Am. Chem. Soc.* **134**, 18843–18852 (2012).

107. Sanchez, P. et al. Ligand protonation at carbon, not nitrogen, during  $\text{H}_2$  production with amine-rich iron electrocatalysts. *Inorg. Chem.* **60**, 17407–17413 (2021).

**Cp ring activation for an amine-rich Cp ligand (that is, not  $\text{Cp}$  or  $\text{Cp}^*$ ) coordinated to an Earth-abundant electrocatalyst for  $\text{H}_2$  production.**

108. Bursch, M., Mewes, J.-M., Hansen, A. & Grimme, S. Best-practice DFT protocols for basic molecular computational chemistry. *Angew. Chem. Int. Ed.* **61**, e202205735 (2022).

109. Kütt, A. et al. Strengths of acids in acetonitrile. *Eur. J. Org. Chem.* **2021**, 1407–1419 (2021).

110. Foster, S. L. et al. Catalysts for nitrogen reduction to ammonia. *Nat. Catal.* **1**, 490–500 (2018).

111. Yandulov, D. V. & Schrock, R. R. Catalytic reduction of dinitrogen to ammonia at a single molybdenum center. *Science* **301**, 76–78 (2003).

112. Arashiba, K., Miyake, Y. & Nishibayashi, Y. A molybdenum complex bearing PNP-type pincer ligands leads to the catalytic reduction of dinitrogen into ammonia. *Nat. Chem.* **3**, 120–125 (2011).

113. Anderson, J. S., Rittle, J. & Peters, J. C. Catalytic conversion of nitrogen to ammonia by an iron model complex. *Nature* **501**, 84–87 (2013).

114. Kuriyama, S. et al. Catalytic transformation of dinitrogen into ammonia and hydrazine by iron-dinitrogen complexes bearing pincer ligand. *Nat. Commun.* **7**, 12181 (2016).

115. Eizawa, A. et al. Remarkable catalytic activity of dinitrogen-bridged dimolybdenum complexes bearing NHC-based PCP-pincer ligands toward nitrogen fixation. *Nat. Commun.* **8**, 14874 (2017).

116. Pappas, I. & Chirik, P. J. Catalytic proton coupled electron transfer from metal hydrides to titanocene amides, hydrazides and imides: determination of thermodynamic parameters relevant to nitrogen fixation. *J. Am. Chem. Soc.* **138**, 13379–13389 (2016).

117. Ashida, Y., Arashiba, K., Nakajima, K. & Nishibayashi, Y. Molybdenum-catalysed ammonia production with samarium diiodide and alcohols or water. *Nature* **568**, 536–540 (2019).

118. Bruch, Q. J. et al. Dinitrogen reduction to ammonium at rhenium utilizing light and proton-coupled electron transfer. *J. Am. Chem. Soc.* **141**, 20198–20208 (2019).

119. Kuriyama, S. et al. Catalytic formation of ammonia from molecular dinitrogen by use of dinitrogen-bridged dimolybdenum-dinitrogen complexes bearing PNP-pincer ligands: remarkable effect of substituent at PNP-pincer ligand. *J. Am. Chem. Soc.* **136**, 9719–9731 (2014).

120. Arashiba, K. et al. Catalytic reduction of dinitrogen to ammonia by use of molybdenum-nitride complexes bearing a tridentate triphosphine as catalysts. *J. Am. Chem. Soc.* **137**, 5666–5669 (2015).

121. Hill, P. J., Doyle, L. R., Crawford, A. D., Myers, W. K. & Ashley, A. E. Selective catalytic reduction of  $\text{N}_2$  to  $\text{N}_2\text{H}_4$  by a simple Fe complex. *J. Am. Chem. Soc.* **138**, 13521–13524 (2016).

122. Chalkley, M. J., Del Castillo, T. J., Matson, B. D., Roddy, J. P. & Peters, J. C. Catalytic  $\text{N}_2$ -to- $\text{NH}_3$  conversion by Fe at lower driving force: a proposed role for metallocene-mediated PCET. *ACS Cent. Sci.* **3**, 217–223 (2017).

**First proposal of ring-activated metallocenes behaving as PCET reagents that contain weak homolytic C–H bonds after protonation.**

123. Chalkley, M. J., Oyala, P. H. & Peters, J. C.  $\text{Cp}^*$  noninnocence leads to a remarkably weak C–H bond via metallocene protonation. *J. Am. Chem. Soc.* **141**, 4721–4729 (2019).

**Unambiguous spectroscopic determination of weak C–H bonds in  $\text{Cp}^*\text{Co}$  and their relevance to PCET chemistry.**

124. Chalkley, M. J., Del Castillo, T. J., Matson, B. D. & Peters, J. C. Fe-mediated nitrogen fixation with a metallocene mediator: exploring  $\text{pK}_a$  effects and demonstrating electrocatalysis. *J. Am. Chem. Soc.* **140**, 6122–6129 (2018).

125. Matson, B. D. & Peters, J. C. Fe-mediated HER vs  $\text{N}_2\text{RR}$ : exploring factors that contribute to selectivity in  $\text{P}_3(\text{E})\text{Fe}(\text{N}_2)$  ( $\text{E} = \text{B}, \text{Si}, \text{C}$ ) catalyst model systems. *ACS Catal.* **8**, 1448–1455 (2018).

126. Garrido-Barros, P., Derosa, J., Chalkley, M. J. & Peters, J. C. Tandem electrocatalytic  $\text{N}_2$  fixation via proton-coupled electron transfer. *Nature* **609**, 71–76 (2022).

127. Harmon, P., Toupet, L., Harmon, J. R. & Lapinte, C. Novel diamagnetic and paramagnetic iron(II), iron(III), and iron(IV) classical and nonclassical hydrides: X-ray crystal structure of  $[\text{Fe}(\text{C}_5\text{Me}_5)_2(\text{dppe})\text{D}]^{\text{PF}_6}$ . *Organometallics* **11**, 1429–1431 (1992).

128. Harmon, P., Harmon, J.-R. & Lapinte, C. Isolation and characterization of a cationic 19-electron iron(III) hydride complex; electron transfer induced hydride migration by carbon monoxide at an iron(III) centre. *J. Chem. Soc. Chem. Commun.* **21**, 1602–1603 (1992).

129. Schild, D. J., Drover, M. W., Oyala, P. H. & Peters, J. C. Generating potent C–H PCET donors: ligand-induced Fe-to-ring proton migration from a  $\text{Cp}^*\text{Fe}(\text{III})\text{H}$  complex demonstrates a promising strategy. *J. Am. Chem. Soc.* **142**, 18963–18970 (2020).

**First account of piano-stool  $\text{Cp}^*\text{Fe}$  complexes that can deliver H atoms via  $\text{Cp}^*$  ring activation.**

130. Wise, C. F., Agarwal, R. G. & Mayer, J. M. Determining proton-coupled standard potentials and X–H bond dissociation free energies in nonaqueous solvents using open-circuit potential measurements. *J. Am. Chem. Soc.* **142**, 10681–10691 (2020).

131. Miller, A. J., Labinger, J. A. & Bercaw, J. E. Trialkylborane-assisted  $\text{CO}_2$  reduction by late transition metal hydrides. *Organometallics* **30**, 4308–4314 (2011).

132. Pitman, C. L., Finster, O. N. & Miller, A. J. Cyclopentadiene-mediated hydride transfer from rhodium complexes. *Chem. Commun.* **52**, 9105–9108 (2016).

**Experimental evidence that ring-activated  $\text{Cp}^*\text{Rh}$  compounds might behave as hydride transfer agents to  $\text{NAD}^+$ .**

133. Pal, S.  $\text{Cp}^*$  non-innocence and the implications of  $(\text{n}^4\text{Cp}^*\text{H})\text{Rh}$  intermediates in hydrogenation of  $\text{CO}_2$ ,  $\text{NAD}^+$ , amino-borane, and the  $\text{Cp}^*$  framework — a computational study. *Dalton Trans.* **52**, 1182–1187 (2023).

134. Kurtz, D. A. et al. Redox-induced structural reorganization dictates kinetics of cobalt(III) hydride formation via proton-coupled electron transfer. *J. Am. Chem. Soc.* **143**, 3393–3406 (2021).

**Evidence supporting that ring-activated  $\text{Cp}$  intermediates precede the formation of  $\text{Co}^{III}\text{H}$  complexes under acidic conditions.**

135. Chalkley, M. J., Garrido-Barros, P. & Peters, J. C. A molecular mediator for reductive concerted proton-electron transfers via electrocatalysis. *Science* **369**, 850–854 (2020).

## Acknowledgements

D.E.P. thanks Rutgers University — Newark and the National Science Foundation (2055097) for support. The authors thank M. Bullock and A. Hansen for constructive comments.

## Author contributions

D.E.P. developed the conceptual framework for this manuscript. All authors contributed to writing and editing the manuscript. All authors reviewed and/or edited the manuscript before submission.

## Competing interests

The authors declare no competing interests.

## Additional information

**Peer review information** *Nature Reviews Chemistry* thanks the anonymous reviewers for their contribution to the peer review of this work.

**Publisher's note** Springer Nature remains neutral with regard to jurisdictional claims in published maps and institutional affiliations.

Springer Nature or its licensor (e.g. a society or other partner) holds exclusive rights to this article under a publishing agreement with the author(s) or other rightsholder(s); author self-archiving of the accepted manuscript version of this article is solely governed by the terms of such publishing agreement and applicable law.

© Springer Nature Limited 2023